

1
2
3
4
5
6
7
8
9
10
11
12
13
14
15
16
17
18
19

**Studying early embryogenesis in the flatworm *Maritigrella*
crozieri indicates a unique modification of the spiral cleavage
program in polyclad flatworms**

Johannes Girstmair^{1,2}, Maximilian J. Telford¹ *

¹ Centre for Life's Origins and Evolution, Department of Genetics, Evolution and Environment,
University College London, London, WC1E 6BT United Kingdom

* corresponding author: m.telford@ucl.ac.uk

² Max Planck Institute of Molecular Cell Biology and Genetics, Pfotenhauerstraße 108, 01307 Dresden,
Germany
girstmair@mpi-cbg.de

20 **Abstract**

21 **Background:** Spiral cleavage is a conserved early developmental mode found in several
22 phyla of Lophotrochozoans with highly diverse adult body plans. While the cleavage pattern
23 has clearly been broadly conserved, it has also undergone many modifications in various taxa.
24 The precise mechanisms of how different adaptations have altered the ancestral spiral
25 cleavage pattern is an important ongoing evolutionary question and adequately answering this
26 question requires obtaining a broad developmental knowledge of different spirally cleaving
27 taxa.

28 In flatworms (Platyhelminthes), the spiral cleavage program has been lost or severely modified
29 in most taxa. Polyclad flatworms, however, have retained the pattern up to the 32-cell stage.
30 Here we study early embryogenesis of the cotylean polyclad flatworm *Maritigrella crozieri* to
31 investigate how closely this species follows the canonical spiral cleavage pattern and to
32 discover any potential deviations from it.

33 **Results:** Using live imaging recordings and 3D reconstructions of embryos, we give a detailed
34 picture of the events that occur during spiral cleavage in *M. crozieri*. We suggest, contrary to
35 previous observations, that the 4-cell stage is a product of unequal cleavages. We show that
36 that the formation of third and fourth micromere quartets are accompanied by strong blebbing
37 events; blebbing also accompanies the formation of micromere 4d. We find an important
38 deviation from the canonical pattern of cleavages with clear evidence that micromere 4d
39 follows an atypical cleavage pattern, so far exclusively found in polyclad flatworms.

40 **Conclusions:** Our findings highlight that early development in *M. crozieri* deviates in several
41 important aspects from the canonical spiral cleavage pattern. We suggest that some of our
42 observations extend to polyclad flatworms in general as they have been described in both
43 suborders of the Polycladida, the Cotylea and Acotylea.

44

45 **Keywords:** Blebbing, Evo-devo, Light-sheet microscopy, Live imaging, Polyclad
46 flatworms, SPIM, Spiralian, Symmetry breaking, Turbellarians

47 **Background**

48

49 The Lophotrochozoa is one of two major clades of protostomes, sister group of the Ecdysozoa,
50 (Aguinaldo et al., 1997; Dunn et al., 2008; Halanych et al., 1995; Hejnol et al., 2009; Pick et
51 al., 2010). It contains approximately a dozen morphologically diverse and mostly marine phyla.
52 While the adult morphology of the different phyla gives few obvious clues as to their close
53 relationships, it has long been recognised that a subset of lophotrochozoan phyla share
54 striking similarities in the earliest events of their embryology, most notably in the spatial
55 arrangement of early blastomere divisions, a developmental mode known as spiral cleavage
56 (Hejnol, 2010; Henry, 2014; Lambert, 2010). Representative lophotrochozoan phyla with spiral
57 cleavage comprise annelids, molluscs, nemertean, flatworms, phoronids and entoprocts
58 (Henry, 2014; Lambert, 2010) and recent phylogenetic results show that these spirally
59 cleaving phyla form a clade within the Lophotrochozoa (Marlétaz et al., 2019). The monophyly
60 of the spirally cleaving phyla strongly suggests a single origin of the spiral cleavage mode.
61 The fact that spiral cleavage has been maintained in these animals since they diverged in the
62 early Cambrian, over half a billion years ago, argues that some selection pressure for
63 maintaining spiral cleavage exists.

64 There are several aspects of spiral cleavage that appear to be highly conserved. The first is
65 the spiral pattern itself: Embryos of the eight-cell stage consist of four larger vegetal
66 macromeres, 1Q, and four smaller animally positioned micromeres, 1q, each sitting skewed
67 to one side of their sister macromere, above the macromeres' cleavage furrows. The typical
68 spiral deformations (SD) of macromeres show a helical twist towards one side with respect to
69 the animal-vegetal axis. This is best seen if the embryo is viewed from the animal pole. The
70 resulting spiral shape taken by all four macromeres is either clockwise (dexiotropic) or counter
71 clockwise (laetropic). In subsequent rounds of division, the larger macromeres again divide
72 unequally and asymmetrically sequentially forming the second and then the third quartets of
73 micromeres. During these divisions the spiral deformations appear in alternating

74 dextrotropic/laetotropic directions (the rule of alternation) up to the fifth cleavage where a 32
75 cell-stage is reached. At this stage, eight cells of each quarter of the embryo can be traced
76 back to one of the large cells at the four-cell stage and constitute the four quadrants, A, B, C
77 and D. This stereotypical production of quartets means that individual blastomeres can be
78 reliably recognised (and arguably therefore homologised) across spiralian phyla through
79 development. To a variable extent, these homologous blastomeres have been shown
80 subsequently to form lineages with similar fates across the Lophotrochozoa (Henry and
81 Martindale, 1998; Henry and Martindale, 1999; Lyons and Henry, 2014)

82 The, four quadrants A, B, C and D, that can be recognized in spirally cleaving embryos, and
83 sometimes individually identifiable as early as the four-cell stage, typically correspond to
84 specific body axes. The D quadrant of spiralian embryos has received particular attention from
85 comparative embryologists - once specified, it is involved in major events of embryonic
86 organization. One D quadrant micromere (typically 4d i.e. the micromere descendant of the
87 4th macromere division) initially and uniquely undergoes a bilaterally symmetrical division
88 determining the dorso-ventral and left right axes of the embryo and then going on to produce
89 large amounts of the future dorsal-posterior part of the embryo. 4d descendants go on to
90 produce endomesoderm (endoderm and mesoderm) (Dorresteijn et al., 1987; Lambert, 2008;
91 Van den Biggelaar and Guerrier, 1983; Verdonk and Van den Biggelaar, 1983). In snails it has
92 been shown that descendants of the D quadrant also possess organizer-like functions
93 (Clement, 1962; Lambert and Nagy, 2001; Martindale, 1986; van den Biggelaar, 1977) The D
94 quadrant lineage arguably holds some of the most conserved features found in spiral cleavers
95 so far.

96
97 While spiral cleavage is generally recognized as homologous and highly conserved across
98 spiralian lophotrochozoans, there are, nevertheless, reports of variations on this conserved
99 theme and even complete loss of this mode of development in different species. Alterations
100 to the spiral cleavage mode include unusual arrangements and differences in relative sizes of
101 blastomeres, alternative cell fates including rare derivations of the otherwise highly conserved

102 origin of the mesoderm (Meyer et al., 2010), and even complete loss of the spiral
103 arrangements of blastomeres (Hejnol, 2010) .

104

105 The mesoderm arises from the D quadrant and, although its lineage is conserved in
106 lophotrochozan development, there are two different ways of specifying which of the four
107 quadrants is the D quadrant. This crucial step can either be achieved early in development
108 by producing blastomeres of different sizes (and presumably containing different maternal
109 transcripts or proteins). Such embryos are classified as “unequal cleavers” whereby the D
110 blastomere at the 4-cell stage is typically the largest cell (Freeman and Lundelius, 1992;
111 Lambert and Nagy, 2003). In other species (equal cleavers), D-quadrant specification is
112 thought to take place by an inductive interaction, usually between one of the large macromeres
113 and the first quartet of micromeres (see Lyons and Henry, 2014). In the latter case, the
114 specification of the D quadrant occurs later in development (Freeman and Lundelius, 1992),
115 with some significant variations in timing.

116

117 To reconstruct the ancestral features of spiral cleavage and to further the understanding of
118 the adaptive basis of any modifications of the spiral cleavage program, it is essential to
119 broaden our knowledge of the phylogenetically conserved and variable features of the spiral
120 cleavage program by studying the full diversity of spiral cleavers. Here we focus on both the
121 conserved and the derived aspects of early spiral cleavage in one important but understudied
122 lophotrochozoan phylum: the Platyhelminthes (flatworms). Across the Platyhelminthes, a wide
123 range of different evolutionary developmental modes is found, indeed, in most members of
124 the phylum spiral cleavage has been lost entirely. Only the Polycladida and its sister group,
125 the Prorhynchida (Egger et al., 2015; Martín-Durán and Egger, 2012), have retained an
126 apparently canonical form of spiral quartet cleavage. For this reason, both taxa are excellent
127 candidates for evolutionary comparative studies (Lapraz et al., 2013; Martín-Durán and Egger,
128 2012).

129 Most of our current knowledge of polyclad embryogenesis derives from observations made in
130 embryos of *Hoploplana inquilina* (Boyer et al., 1998; Surface, 1907), which belongs to the
131 Acotylea, one of the two major suborders found within polyclad flatworms. Here, we
132 investigate the early cleavages of *Maritigrella crozieri* a member of the Cotylea - the second
133 major clade of polyclads. *Maritigrella* has been recently introduced as a model to study
134 flatworm evolution and development (Girstmair et al., 2016; Lapraz et al., 2013; Rawlinson,
135 2010). We provide the most detailed description to date of the early development of a cotylean
136 polyclad flatworm. To visualize the development of embryos *in vivo* we used a recently
137 established live-imaging setup, using selective plane illumination microscopy (SPIM) via the
138 OpenSPIM open access platform (Gualda et al., 2013; Pitrone et al., 2013), which allows *in*
139 *vivo* recordings and precise 3D reconstructions of polyclad flatworm embryos (Girstmair et al.,
140 2016). We use 4D live imaging to visualize details of the early development of *M. crozieri* and
141 we examine cell volume measurements of blastomeres from the first and second cleavages.
142 Live imaging also allows us to make new observations of blastomere dynamics during spiral
143 quartet cleavage.

144

145 **Results and Discussion**

146 **Overview of the spiral cleavage pattern in *Maritigrella crozieri***

147 The development of polyclad flatworms closely follows the conserved spiral cleavage mode
148 and this is true of both polyclad suborders, the Acotylea and Cotylea, as well as in direct and
149 indirect developers within both suborders (Boyer et al., 1998; Gammoudi et al., 2011; Goette,
150 1881; Kato, 1940; Lang, 1884; Lapraz et al., 2013; Malakhov and Trubitsina, 1998; Martín-
151 Durán and Egger, 2012; Rawlinson, 2010; Surface, 1907; Wilson, 1898). Cleavage in
152 polyclads, as in other spiralian, begins with two meridional divisions (from animal pole to
153 vegetal pole) resulting in four cells arranged around the central animal-vegetal axis and these
154 blastomeres have the standard names of A, B, C, D. The stereotypical polyclad cleavage
155 pattern after the four-cell stage from the third to the fifth cleavage (32-cell stage) is
156 summarized in Figure 1, A-C. Thereby three quartets of ectodermal micromeres (1q-3q) are
157 budded at the animal pole by repeated divisions of the large macromeres. In most spiral
158 cleavers a fourth and sometimes even a fifth quartet of blastomeres are formed in this specific
159 geometry. In polyclad flatworms, however, the fourth quartet significantly deviates from the
160 stereotypic cleavage in terms of both relative size of micromeres and macromeres and their
161 orientation. In contrast to the formation of the first three quartets of micromeres, the fourth
162 quartet 'micromeres' are considerably larger than the four sister 'macromeres' which form as
163 four tiny cells at the vegetal pole (see Figure 1 D). This unusual characteristic of large 4th
164 quartet micromeres has been previously shown in polyclad flatworms including both *H.*
165 *inquilina* (Boyer et al., 1998) and *M. crozieri* (Rawlinson, 2010).

166

167 Our observations of *M. crozieri's* earliest cleavage pattern, which include live-imaging
168 recordings (Figure 2) and scanning electron microscopy images (Figure 3, A-F) are in
169 accordance with previous 4D recordings up to the 16-cell stage (Lapraz et al., 2013) and
170 descriptions of fixed specimens (Rawlinson, 2010). In some specimens we noted that second
171 cleavages were slightly asynchronous, which explains the occasional observation of embryos

172 in a 3-cell stage before the formation of four similarly sized blastomeres takes place. The
173 characteristic cleavage pattern and spiral deformations are prominent; the 4- to 8-cell
174 transition is dextrotropic (compare Figure 1, A Figure 3, A and Additional file 1). As the division
175 of the first quartet micromeres (1a-1d) is slightly delayed relative to the division of their sister
176 macromeres (1A-1D), an intermediate 12-cell stage forms (Figure 3, C and D). During the
177 generation of new quartets by division of macromeres, the micromeres of the existing quartets
178 also divide and, after the third quartet is completed, the embryo reaches a 32-cell stage.

179

180 We suggest that, during the polyclad-specific fourth quartet formation, the unusual asymmetric
181 division resulting in large micromeres and small macromeres is achieved in part by a
182 significant displacement of the nuclei in all four macromeres (3Q) prior to their division as is
183 shown here in embryos of *M. crozieri* (Figure 3, G-J). The macromere nuclei, which are
184 typically placed towards the animal pole, shift significantly towards the vegetal pole in 3A-3D
185 (Figure 3, G and H, blue arrows). As a result of these movements, the nuclei of 3A-3D meet
186 at the vegetal pole of the embryo, just before the macromeres divide (Figure 3, I, purple
187 nuclei). The newly formed large micromeres retain most of their size and all the yolk. After the
188 completion of the fourth quartet of micromeres, embryos have reached the 36-cell stage. In
189 polyclads, except for micromere 4d, cells of the fourth quartet do not appear to undergo any
190 further divisions for as long as they can be traced during epibolic gastrulation (Boyer et al.,
191 1998; Rawlinson, 2010; Surface, 1907). At the point when cilia form on the epidermis and
192 embryos start to rotate, cells become difficult to identify and their fates obscure, however,
193 there is evidence from our live imaging recordings that, during epiboly and after bilateral
194 symmetry is established, these small macromeres could engage in further cell-cell
195 interactions. The nuclei of the small macromeres (4A-4D) can be seen in close proximity with
196 nuclei of descendants of micromere 4d¹ (probably micromere 4d¹¹) as is shown in Figure 4
197 and as a movie (see Additional file 2). This observation suggests that the fourth quartet
198 macromeres undergo later cell interactions and this might play a more important
199 developmental role than has previously been appreciated.

200

201 The dramatic changes in cell behaviour from an animally-positioned cleavage position into a
202 vegetal one resulting in small ‘macromeres’ of the fourth quartet are not widely observed in
203 other spirally cleaving embryos. This deviation from typical quartet formation pattern raises
204 the question as to how and why such a modification evolved. Interestingly, in the common
205 bladder snail *Physa fontinalis* the fourth quartet emerges in a very similar way to polyclad
206 flatworms, producing a rosette of four smaller macromeres (4A-4D) at the most vegetal pole
207 and four larger micromeres (4a-4d) above it (Wierzejski, 1905). In *P. fontinalis*, unlike polyclad
208 flatworms, macromere 3D divides earlier in the snail than its sister cells (3A-3C) giving rise to
209 micromere 4d (the mesentoblast). Furthermore, in *P. fontinalis*, cells of the small macromere
210 rosette (4A-4D) undergo a further division producing a fifth quartet of micromeres through
211 equal divisions of 4A-4C.

212 **The four-cell stage is a product of asymmetric cleavages in *M. crozieri***

213 In spiral cleavers, equal and unequal cleavage types can be readily distinguished during the
214 first two divisions. The cleavage mode has been thought to reflect the way in which the embryo
215 determines one of its four quadrants to become designated as the D quadrant. (Arnolds et al.,
216 1983; Martindale et al., 1985; van den Biggelaar, 1996; van den Biggelaar and Guerrier,
217 1979). As the D quadrant plays a major developmental role in the developing embryo, we
218 wanted to measure the relative sizes of blastomeres in *Maritigrella*, in particular after the
219 second cleavage takes place. Polyclad flatworms, including *M. crozieri*, have been considered
220 equal cleavers on the basis of their indistinguishable relative blastomere sizes at the 2- and
221 4-cell stages (Lapraz et al., 2013; Martín-Durán and Egger, 2012; Rawlinson, 2010). To test
222 this in *Maritigrella*, we performed a series of precise blastomere volume measurements during
223 the first and second cleavages. We 3D reconstructed 25 fixed embryos between the 2- and 4-
224 cell stages. Additional file 3 (A-E and A'-E') depicts how the precise volume of given
225 blastomeres can be measured manually using an open source Fiji-plugin (Volumest;

226 <http://lepo.it.da.ut.ee/~markkom/volumest/>). The measurement data of individual blastomeres
227 can be seen in Additional file 4. For convenience and easier comparison, we labeled vegetal
228 cross-furrow cells in *M. crozieri* as B and D of which the larger cell was always designated as
229 D. Accordingly, the remaining cells were labelled as A and C in consideration of the dextral
230 cleavage type present in *M. crozieri*. One should keep in mind that this assignment may not
231 represent the true quadrants (Rawlinson, 2014) but this process allows us to see at least if
232 there is a consistently larger blastomere and, if so, whether this is an animal or vegetal cross
233 furrow cell.

234 A small but consistent volume difference of 6% ($\pm 1.6\%$) on average could be discerned
235 between the two blastomeres at the 2-cell stage ($n=13$) (Figure 5, F and Additional file 4). Two
236 embryos of a transient 3-cell stage show that volumes of the two sister cells also differ (Figure
237 5, G and Additional file 5) and together have a larger volume than the remaining third
238 blastomere. In the four cell stages, in 9/10 cases, the vegetal cross furrows of the
239 reconstructed embryos were clearly identifiable as schematically drawn in Figure 5, B and
240 depicted in Figure 5, F and F'. Measuring individual blastomeres of 4-cell stage embryos ($n =$
241 10) indicates that one of the four cells is larger than the others (Figure 5, F and Additional file
242 5). This is unlikely to be a random effect as whenever vegetal cross-furrows of 4-cell stage
243 embryos are recognizable, the cell with the largest volume can be identified as one of these.
244 Based on these measurements, *M. crozieri* undergoes asymmetric cell divisions during the
245 first and second cleavages, although they are more pronounced during the two to four-cell
246 transition.

247

248 Understanding whether a spiralian embryo is an unequal or equal cleaver is important as it
249 has major implications for determining the mechanism of D quadrant specification. In unequal
250 cleavers (with unequal sized blastomeres at the 4-cell stage), the D quadrant (and therefore
251 the dorsal-ventral axis) can be determined as early as the 4-cell stage: it is assumed that a
252 differential distribution of maternal factors takes place during the first two divisions coinciding
253 with a noticeable inequality of the size of the large D blastomere in comparison to blastomeres

254 A-C (Astrow et al., 1987; Cather and Verdonk, 1979; Clement, 1952; Dorresteyn et al., 1987;
255 Henry, 1986; Henry, 1989; Henry and Martindale, 1987; Render, 1983; Render, 1989).

256

257 D-quadrant specification in equal cleavers requires an inductive interaction, usually between
258 one of the equal sized, large vegetal macromeres and the first quartet of micromeres
259 positioned at the animal pole. So far, *H. inquilina* is the only polyclad flatworm where earlier
260 blastomere deletion experiments indicated that, in 2-cell and 4-cell stage embryos,
261 asymmetrically distributed morphogenetic determinants could be involved in development
262 (Boyer, 1987) as expected of an unequal cleaver. There is also evidence, however, for the
263 importance of cell-cell interactions between macromeres and micromeres in *H. inquilina* as is
264 typical of equal cleavers (Boyer, 1989).

265

266 Our volume measurements indicate that *M. crozieri* does not follow an equal cleavage pattern,
267 although the differences in blastomere size are relatively subtle. At the same time, it is too
268 early to suggest a strictly unequal cleavage mode. It remains possible that there are additional
269 inductive events occurring later in embryogenesis as noted in *H. inquilina*. These could be
270 important for the D quadrant specification and might not be readily observable on a
271 morphological level. In the snail *Illyanassa obsoleta* a mechanism for asymmetric messenger
272 RNA segregation by centrosomal localization during cleavage has been described (Lambert,
273 2009). It would be very interesting to test for a similar molecular mechanism in polyclad
274 flatworms and to screen for components that play a crucial role in asymmetric cell division
275 machinery as has been recently performed in the spiral cleaving embryo *Platynereis dumerilii*
276 via RNA sequencing (Nakama et al., 2017).

277

278

279

280 **Micromere 4d in *M. crozieri* shows a cleavage pattern unique to polyclad**
281 **flatworms**

282 In embryos with spiral cleavage, micromere 4d typically divides into a left and a right daughter
283 cell by a meridional division. It is at this point that the bilateral symmetry of the embryo first
284 emerges at a cellular level. To determine the symmetry breaking event during *M. crozieri*
285 development we followed the division pattern of micromere 4d using our live-imaging data.
286 We observe that the 4d blastomere in *M. crozieri* does not divide meridionally into a left and
287 right daughter cell, but first divides along the animal-vegetal axis into a smaller, animally
288 positioned cell, which we designate as 4d² and a larger, vegetally positioned cell, we designate
289 4d¹ (Figure 6, A-B and F-H; Additional file 6). We thereby follow closely the nomenclature used
290 by Surface (1907) and it should be noted that in this specific case (the animal-vegetal division
291 of an ento- and mesoblast and not the ectoblast) the smaller exponent was intentionally
292 reserved for the more vegetally positioned “parent” cell. Only following this additional division
293 of micromere 4d, is definitive bilateral symmetry established by the meridional (left-right)
294 division of both sister cells, 4d¹ and 4d² (Figure 6, C-E and H-J). The meridional divisions of
295 4d¹ and 4d² appear equal and this equality is easily observed in 4d² due to its larger size and
296 exposed external position. Both descendants of 4d¹ and 4d² (4d¹¹ and 4d¹² and 4d²¹ and 4d²²)
297 then undergo another round of roughly meridional cleavages. This is similar to Surface’s
298 descriptions in *H. inquilina* (Surface, 1907).

299 Surface (1907) and later van den Biggelaar (1996) both already noted that in polyclads the
300 cleavage of 4d differs from the canonical pattern of an immediate, equal and meridional
301 division into left and right descendants. According to van den Biggelaar, in the polyclads
302 *Hoploplana inquilina* and *Prostheceraeus giesbrechtii*, this meridional division is delayed by
303 one cell cycle as 4d first undergoes the approximately animal-vegetal division into 4d¹ and
304 4d². This is followed by meridional cleavages of both daughter cells 4d¹ and 4d². These
305 observations exactly match what we observe in *M. crozieri*. In other more recent descriptions
306 of polyclad flatworms (Hartenstein and Ehlers, 2000; Malakhov and Trubitsina, 1998;

307 Rawlinson, 2010; Teshirogi et al., 1981; Younossi-Hartenstein and Hartenstein, 2000), this
308 the animal-vegetal division of 4d is not mentioned suggesting either that some polyclad
309 flatworms lack it or, more likely, that the division is difficult to observe without continuous
310 recording. Our observations in the *M. crozieri* together with description of *H. inquilina* by
311 Surface and *P. giesbrechtii* by Van den Biggelaar strongly suggests that this cleavage pattern
312 of micromere 4d is in fact unique amongst spiralian but common across polyclads.

313 **Post-meiotic protrusions of the cell membrane (blebbing) accompany early**
314 **development in *M. crozieri***

315 In several animal phyla, oocytes undergo cytoplasmic changes that are capable of temporarily
316 deforming the shape of the egg and which have been suggested as a sign of the oocyte
317 segregating cell content (Wall, 1990). Such events have been commonly observed during
318 fertilization and meiosis (Henry et al., 2006; Lehmann and Hadorn, 1946; Li and Albertini,
319 2013; Meshcheryakov, 1991). In polyclads this has been demonstrated many times previously
320 and is referred to as cell blebbing (Anderson, 1977; Gammoudi et al., 2011; Goette, 1881;
321 Hallez, 1879; Kato, 1940; Malakhov and Trubitsina, 1998; Rawlinson et al., 2008; Selenka,
322 1881; Surface, 1907; Teshirogi et al., 1981; Younossi-Hartenstein and Hartenstein, 2000). It
323 has occasionally been noted that cell-blebbing is not restricted to egg maturation and the
324 extrusion of the polar bodies but can reappear frequently during early cleavages ((Gammoudi
325 et al., 2012; Malakhov and Trubitsina, 1998; Teshirogi et al., 1981).

326 In *M. crozieri*, our observations show that blebbing during egg maturation follows first a
327 depression of the oocyte at the animal pole (Figure 7, A) followed by protrusions all over the
328 cell membrane (Figure 7, C and insets). These events are almost identical to drawings of egg
329 maturation and oocyte blebbing based on different Japanese polyclad species by Kato (1940).

330

331 Blebbing in *Maritigrella* continues after meiosis, specifically during the asymmetric cleavages
332 of macromeres (Figure 7). The formation of the third and fourth quartet micromeres is clearly

333 accompanied by strong blebbing events in the macromeres distinct from what is seen in
334 meiotic cell blebbing (Figure 7, E-L). In the case of the third quartet formation we observe that,
335 prior to the cleavage of macromeres 2A-2D, blebbing becomes visible on their cell surfaces in
336 form of small, vesicle-like protrusions (Figure 7, E-H) (n = 17/18). The role of these vesicles is
337 not clear, but we can observe that mitotic cytoskeletal activity during anaphase correlates with
338 the observed protrusions (Additional file 7 and Additional file 8). In contrast, during the
339 formation of the fourth quartet (3A- 3D), cytoplasmic perturbations create waves of contractile
340 activity with smaller blebs that appear more frequently. In this case, the macromeres can
341 sometimes attain an elongated shape (Figure 7, I-L) (n=18/18) at the onset of the formation of
342 micromeres 4a-4d. More detailed time-lapse sequences of these peculiar cytoplasmic
343 perturbations are shown in Additional file 9. Finally, the asymmetric division of micromere 4d
344 in *M. crozieri* is also accompanied by distinctive cytoplasmic perturbations of the membrane
345 (Figure 7, M-P and M'-P'); n = 16/16). The perturbations of micromere 4d mark the end of a
346 series of cell shape changes visible throughout early development. In Figure 8 we summarise
347 the events previously described in polyclad flatworms, together with our own observations of
348 the early development of *M. crozieri*.

349

350 At present it is unclear what role (if any) post-meiotic blebbing plays during early cleavage. It
351 is interesting to see that the perturbations observed in *Maritigrella* during divisions of
352 macromeres 2A-2D (extracellular vesicle-like structures; see Figure 7, E-H) look identical to a
353 highly similar blebbing event in another polyclad species, the acotylean *Pseudostylochus*
354 *intermedius* (Teshirogi et al., 1981), although in the latter species this phenomenon is
355 described to take place one division round earlier (8- to 16-cell stage). Blebbing during the
356 divisions of macromeres 3A-3D and the division of micromere 4d are both described by us for
357 the first time during polyclad embryogenesis.

358 One observation suggesting blebbing has an important function in polyclad embryogenesis is
359 that when embryos are mounted in high concentrations of agarose (>0.6%) we observed

360 severely abnormal development (n=5/5). We speculate that these defects may be caused by
361 blebbing being hampered by the stiff agarose. Common to all of the blebbing events is that
362 they occur in cells which contain most of the yolk and which undergo asymmetric divisions.
363 Additionally, we show here that they coincide with increased cytoskeletal activity (mitosis).
364 One simple explanation for their occurrence may be that they are the visible manifestation of
365 actomyosin contractions of the cortex during strong cytoskeletal movements involved in
366 asymmetric cleavage in yolk-rich blastomeres.

367 **Conclusions**

368 In this study we have used live-imaging recordings and 3D reconstructions to extend
369 observations of early development in a cotylean polyclad flatworm, *Maritigrella crozieri*. 3D
370 reconstructions and continuous 4D recordings allow us to see developmental events in more
371 detail than previously possible. We have been able to look at connections between nuclear
372 movements and cell divisions and link them with cellular dynamics such as cell blebbing
373 (protrusions of the membrane), and pinpoint important developmental events like symmetry
374 breaking. Our observations allow us to confirm and extend previous developmental
375 observations of early embryogenesis in polyclads, made using fixed specimens, describing
376 the spiral cleavage pattern and the formation of the four quartets. There seems to be little
377 variation within both polyclad suborders, the cotyleans and the acotyleans.

378
379 One important observation in *M. crozieri* is that this so-called equal cleaving polyclad should
380 probably not be classified as such. Our measurements of individual blastomeres at the 4-cell
381 stage show that the second cleavage is a product of unequal divisions of which one vegetal
382 cross-furrow blastomere retains the largest volume. Similar observations of unequal cleavage
383 may be a broader pattern within polyclads, including species so far regarded as “equal”
384 cleavers, but requires precise measurements to be carried out in different species. In *M.*

385 *crozieri* the question remains as to whether the observed size differences at the 4-cell stage
386 truly reflect an unequal cleavage mechanism, meaning that the D quadrant is already specified
387 by maternal determinants at this early stage. Clearly, we need to know more about the
388 molecular basis of putative maternal determinants and the mechanisms by which they could
389 be sequestered but an early specification of the D quadrant via cytoplasmic localization seems
390 to be supported by previous studies on *Hoploplana inquilina* (Boyer, 1987; Boyer, 1989).

391

392 Most importantly, we found that the animal-vegetal division of micromere 4d is present in both
393 polyclad suborders, and we suggest this is a conserved pattern across all polyclad flatworms.
394 It would be highly interesting to reinvestigate this cleavage pattern within the Prorhynchida,
395 where the spiral cleavage pattern with quartet formation has also been partly retained but
396 current developmental data are insufficient to conclude whether it follows the pattern as
397 suggested for polyclads in this study.

398 We consider that the exact fate of both daughter cells of micromere 4d must be investigated
399 more thoroughly before we can conclude whether micromere 4d² (animally positioned relative
400 to 4d¹) indeed represents the mesentoblast or not. Currently, even the fate of 4d¹, despite its
401 large size and the fact that it is readily visible at the onset of gastrulation, remains unclear, as
402 model lineage tracing of this specific blastomere has not been yet performed. This could be
403 done by Dil injections or perhaps via fluorescently tagged and photoconvertible molecules. It
404 would also be interesting to study further the apparent interaction of one of the daughter cells
405 4d¹ with small macromeres (4A-D), observed during our live-imaging recordings in *M. crozieri*,
406 as this is the first time that cell-cell interactions may have been directly identified in a polyclad
407 flatworm and that a potentially significant developmental role is assigned to the small
408 macromeres.

409

410 We show here new evidence that, in *M. crozieri*, blebbing is present not only in oocytes during
411 meiosis, but also in macromeres during quartet formation and in micromere 4d during its first
412 cleavage along the animal-vegetal axis (Figure 6, Figure 7 and Additional file 6). We propose

413 that it is likely that these are a manifestation of the mechanical forces created by cytoskeletal
414 dynamics during early cleavages, which may be more or less obvious depending on the
415 polyclad species and the amount of yolk within the blastomere. Alternatively, these
416 movements could fulfill other purposes such as correctly sequestering factors that could play
417 a role in development, but this remains to be seen in future studies.

418

419 Taken together the most crucial events during polyclad spiral cleavage take place as follows:
420 Firstly a D quadrant might be established as early as the 4-cell stage by cytoplasmic
421 localizations (Boyer, 1989). The atypical formation of the fourth quartet then gives rise to
422 micromere 4d, which arguably behaves similarly to macromere 3D in molluscan and annelid
423 embryos (van den Biggelaar, 1996). Unusually, micromere 4d undergoes an animal-vegetal
424 division, which buds micromere 4d² into the interior of the embryo and in proximity to the
425 animal cap as shown by Surface (1907) in *H. inquilina* and *M. crozieri* (this study). In our
426 opinion the position 4d² assumes during this event allows it the possibility to interact with
427 micromeres of the first quartet. Such animal-vegetal inductive interactions are typically
428 observed in equally cleaving spiralian (Lyons and Henry, 2014) and could also play a crucial
429 role in polyclads in terms of specifying the D quadrant. Ultimately, 4d² may be considered the
430 mesentoblast (Martín-Durán and Egger, 2012), but this still remains to be determined more
431 carefully.

432

433 As shown in this work, polyclad flatworms appear to combine conserved features of spiral
434 cleavage but also show obvious modifications of their cleavage program. This makes them a
435 highly interesting taxa for evolutionary comparisons among flatworms within and outside the
436 polyclad order but also across lophotrochozoan phyla. Live imaging recordings such as SPIM
437 can certainly contribute also in future studies to extend our current understanding of polyclad
438 development and other marine invertebrates.

439 **Methods**

440 **Animal culture**

441 Adult specimens of *M. crozieri* were collected in coastal mangrove areas in the Lower Florida
442 Keys, USA in January 2014, November 2014 September 2015 and January 2016 near Mote
443 Marine Laboratory (24.661621, -81.454496). Animals were found on the ascidian
444 *Ecteinascidia turbinata* as previously described (Lapraz et al., 2013). Eggs without egg-shells
445 (to produce 'naked' embryos) were obtained from adults by poking with a needle (BD
446 Microlance 3) and raised in Petri dishes coated with 2% agarose (diluted in filtered artificial
447 seawater) or gelatin coated Petri dishes at room temperature in penicillin-streptomycin (100
448 µg/ml penicillin; 200 µg/ml streptomycin) treated Millipore filtered artificial seawater (35-36 ‰).

449

450 ***In vitro* synthesis of mRNA**

451 We synthesised mRNAs for microinjections with Ambion's SP6 mMACHINE kit.
452 The capped mRNAs produced were diluted in nuclease-free water and used for
453 microinjections in order to detect fluorescence signal in early *M. crozieri* embryos. Nuclei were
454 marked and followed using histone H2A-mCherry (H2A-mCh) and GFP-Histone (H2B-GFP).
455 The plasmids carrying the nuclear marker pCS2-H2B-GFP (GFP-Histone) and pDestTol2pA2-
456 H2A-mCherry (Kwan et al., 2007) were transformed, purified and concentrated as described
457 before and then linearized with the restriction enzymes NotI and BglII respectively. To follow
458 live microtubules, we used a GFP fusion of the microtubule binding domain of ensconsin
459 (EMTB-3XGFP). These clones were the gift of the Bement Lab (University of Wisconsin)
460 (Burkel et al., 2007; Miller and Bement, 2009) and were commercially ordered from
461 <http://addgene.org> (EMTB-3XGFP: <https://www.addgene.org/26741/>).

462

463

464

465 **Microinjections**

466 Fine-tipped microinjection needles were pulled on a Sutter P-97 micropipette puller
467 (parameters: P=300; H=560; Pu=140; V=80; T=200.) and microinjections of synthesized
468 mRNA (~300-400 ng/μl per mRNA in nuclease-free water) were carried out under a Leica
469 DMI3000 B inverted scope with a Leica micromanipulator and a Picospitzer® III at room
470 temperature.

471

472 **4D microscopy of live embryos using OpenSPIM**

473 Embryos showing fluorescent signal were selected under an Axioimager M1 Epifluorescence
474 and Brightfield Microscope (Zeiss). Live embryos were briefly incubated in 40 °C preheated
475 and liquid low melting agarose (0.1%) and immediately sucked into fluorinated ethylene
476 propylene (FEP) tubes (Bola S1815-04), which were mounted in the OpenSPIM acquisition
477 chamber which was filled with filtered artificial seawater and antibiotics via a 1 ml BD
478 Plastikpak (REF 300013) syringe. The use of FEP tubes has been previously described
479 (Kaufmann et al., 2012) and allows the specimen to remain inside the tube during image
480 acquisition without causing any blurring to the acquired images, as would be the case with
481 other mounting materials such as glass capillaries. Using FEP tubes enables us to mount
482 specimens in lower percentage agarose (0.1-0.2%), thus lessening the perturbation of embryo
483 growth and development. The interval between images depends on the user's intentions.
484 Long-term imaging single timepoints can consist of 40-70 optical slices and were captured
485 every 1-3 minutes. The OpenSPIM was assembled according to our previous description
486 (Girstmair et al., 2016) and operated using MicroManager (version 1.4.19; November 7, 2014
487 release; <https://www.micro-manager.org/>).

488 **4D microscopy of live embryos under an Axio Zoom.V16 (Zeiss)**

489 Several embryos in which fluorescent signal could be detected were centered within a 90 mm
490 petri dish containing penicillin-streptomycin (100 μg/ml penicillin; 200 μg/ml streptomycin)

491 treated Millipore filtered artificial seawater (35-36 ‰) for simultaneous live imaging. To avoid
492 evaporation and make fluorescent imaging possible a tiny hole was made in the middle of the
493 lid and artificial seawater containing fresh antibiotics carefully exchanged from the side when
494 evaporation became apparent. Brightfield, green and red fluorescence was acquired every 5-
495 7 min.

496

497 **Fixation and imaging of embryos used for scanning electron microscopy (SEM)**

498 Batches of embryos were raised until development reached the desired stage (1-cell, 2-cell,
499 4-cell, 8-cell, 16-cell, 32-cell, 64-cell and intermediate phases). Fixation was done at 4°C for
500 1 hour in 2.5% glutaraldehyde, buffered with phosphate buffered saline (PBS; 0.05 M PB/0.3
501 M NaCl, pH 7.2) and post-fixed at 4°C for 20 min in 1% Osmium tetroxide buffered with PBS.
502 Fixed specimens were dehydrated in an ethanol series, dried via critical point drying, and
503 subsequently sputtered coated with carbon or gold/palladium in a Gatan 681 High Resolution
504 Ion Beam Coater and examined with a Jeol 7401 high resolution Field Emission Scanning
505 Electron Microscope (SEM).

506

507 **Fixation and staining of embryos for 3D reconstruction**

508 Embryos were extracted from gravid adults at the Keys Marine Laboratory (Florida) by poking
509 and allowed to cleave until the desired stage was reached. Embryos were then fixed for 60
510 min in 4 % formaldehyde (from 16 % paraformaldehyde: 43368 EM Grade, AlfaAesar) in PBST
511 (0.1 M phosphate buffer saline containing 0.1% Tween 20) at room temperature, followed by
512 a 5x washing step in PBST and stored at 4 °C in PBST containing small concentrations of
513 sodium azide.

514 In order to image specimens from 5 angles, which is necessary to perform volume
515 measurements of early blastomeres, sodium azide with 0.1 M PBS containing 0.1% Triton X-
516 100 in (PBSTx) was washed off fixed embryos by four washing steps and stained with 1:300
517 Rhodamine Phalloidin (ThermoFisher Scientific R415) for 2-3 h at room temperature or

518 overnight at 4°C. Following several washes of PBST or PBSTx 0.1 µM of the nuclear stain
519 SytoxGreen (Invitrogen), which is difficult to detect at these early stages, was added for 30
520 min and the embryos then rinsed with PBST for another hour.

521

522 **Image processing**

523 Post-processing of acquired data was performed with the latest version of the freely available
524 imaging software Fiji (Schindelin et al., 2012) and digital images were assembled in Adobe
525 Photoshop CC 2017.

526

527 **Ethics approval and consent to participate**

528 Not applicable.

529

530 **Consent for publication**

531 Not applicable.

532

533 **Availability of data and materials**

534 The datasets during and/or analysed during the current study available from the corresponding
535 author on reasonable request.

536

537 **Competing interests**

538 The authors declare that they have no competing interests.

539

540 **Funding**

541 JG was funded by the Marie Curie ITN 'NEPTUNE' grant (no. 317172), under the FP7 of the
542 European Commission. M.J.T. was supported by the European Research Council (ERC-2012-
543 AdG 322790), the Biotechnology and Biological Sciences Research Council grant
544 (BB/H006966/1 and a Royal Society Wolfson Research Merit Award.

545

546 **Author contributions**

547 MJT and JG designed the experiments. JG performed all the experiments and prepared the
548 figures. JG and MJT analysed the data and wrote the manuscript. The authors read and
549 approved the final manuscript.

550

551 **Acknowledgements**

552 We thank Anne Zakrzewski for her help with scanning electron microscopy pictures, Bernhard
553 Egger and Kate Rawlinson for their continuous support and helpful discussions, Fraser
554 Simpson for his immense effort during the Florida collection trips, the Mote Marine Laboratory
555 (<https://mote.org/>) and Keys Marine Laboratory (<http://www.keysmarinelab.org/>) for their
556 support during our stay in the Florida Keys.

557

558 **REFERENCES**

- 559 **Aguinaldo, A. M. A., Turbeville, J. M., Linford, L. S., Rivera, M. C., Garey, J. R., Raff, R. A. and Lake, J.**
560 **A.** (1997). Evidence for a clade of nematodes, arthropods and other moulting animals. *Nature*
561 **387**, 489–493.
- 562 **Anderson, D. T.** (1977). The embryonic and laval development of the turbellarian *Notoplana australis*
563 (Schmarda, 1859) (Polycladida: Leptoplanidae). *Mar. Freshw. Res.* **28**, 303–310.
- 564 **Arnolds, W. J. A., van den Biggelaar, J. A. M. and Verdonk, N. H.** (1983). Spatial aspects of cell
565 interactions involved in the determination of dorsoventral polarity in equally cleaving gastropods
566 and regulative abilities of their embryos, as studied by micromere deletions in *Lymnaea* and
567 *Patella*. *Wilhelm Roux's Arch. Dev. Biol.* **192**, 75–85.
- 568 **Astrow, S., Holton, B. and Weisblat, D.** (1987). Centrifugation redistributes factors determining
569 cleavage patterns in leech embryos. *Dev. Biol.* **120**, 270–283.
- 570 **Boyer, B. C.** (1987). Development of in vitro fertilized embryos of the polyclad flatworm, *Hoploplana*
571 *inquilina*, following blastomere separation and deletion. *Roux's Arch. Dev. Biol.* **196**, 158–164.
- 572 **Boyer, B. C.** (1989). The Role of the First Quartet Micromeres in the Development of the Polyclad
573 *Hoploplana inquilina*. *Biol. Bull.* **177**, 338–343.
- 574 **Boyer, B. C., Henry, J. Q. and Martindale, M. Q.** (1996). Dual origins of mesoderm in a basal spiralian:
575 cell lineage analyses in the polyclad turbellarian *Hoploplana inquilina*. *Dev. Biol.* **179**, 329–338.
- 576 **Boyer, B. C., Henry, J. Q. and Martindale, M. Q.** (1998). The cell lineage of a polyclad turbellarian

- 577 embryo reveals close similarity to coelomate spiralian. *Dev. Biol.* **204**, 111–123.
- 578 **Burkel, B. M., Von Dassow, G. and Bement, W. M.** (2007). Versatile fluorescent probes for actin
579 filaments based on the actin-binding domain of Utrophin. *Cell Motil Cytoskelet.* **64**, 822–832.
- 580 **Cather, J. N. and Verdonk, N. H.** (1979). Development of *Dentalium* following removal of D-quadrant
581 blastomeres at successive cleavage stages. *Wilhelm Roux's Arch. Dev. Biol.* **187**, 355–366.
- 582 **Clement, A. C.** (1952). Experimental studies on germinal localization in *Ilyanassa*. I. The role of the
583 polar lobe in determination of the cleavage pattern and its influence in later development. *J. Exp.*
584 *Zool.* **121**, 593–625.
- 585 **Clement, A. C.** (1962). Development of *Ilyanassa* following removal of the D macromere at successive
586 cleavage stages. *J. Exp. Zool.* **149**, 193–215.
- 587 **Dorresteijn, A. W. C., Bornewasser, H. and Fischer, A.** (1987). A correlative study of experimentally
588 changed first cleavage and Janus development in the trunk of *Platynereis dumerilii* (Annelida,
589 Polychaeta). *Roux's Arch. Dev. Biol.* **196**, 51–58.
- 590 **Dunn, C. W., Hejnol, A., Matus, D. Q., Pang, K., Browne, W. E., Smith, S. A., Seaver, E., Rouse, G. W.,**
591 **Obst, M., Edgecombe, G. D., Sørensen, M. V, Haddock, S. H. D., Schmidt-Rhaesa, A., Okusu, A.,**
592 **Kristensen, R. M., Wheeler, W. C., Martindale, M. Q. and Giribet, G.** (2008). Broad
593 phylogenomic sampling improves resolution of the animal tree of life. *Nature* **452**, 745–749.
- 594 **Egger, B., Lapraz, F., Tomiczek, B., Müller, S., Dessimoz, C., Girstmair, J., Škunca, N., Rawlinson, K.**
595 **A., Cameron, C. B., Beli, E., Todaro, M. A., Gammoudi, M., Noreña, C. and Telford, M. J.** (2015).
596 A transcriptomic-phylogenomic analysis of the evolutionary relationships of flatworms. *Curr.*
597 *Biol.* **25**, 1347–1353.
- 598 **Freeman, G. and Lundelius, W. J.** (1992). Evolutionary implications of the mode of D quadrant
599 specification in coelomates with spiral cleavage. *J. Evol. Biol.* **5**, 205–247.
- 600 **Gammoudi, M., Noreña, C., Tekaya, S., Prantl, V. and Egger, B.** (2011). Insemination and embryonic
601 development of some Mediterranean polyclad flatworms. *Invertebr. Reprod. Dev.* **56**, 272–286.
- 602 **Gammoudi, M., Egger, B., Tekaya, S. and Noreña, C.** (2012). The genus *Leptoplana* (Leptoplanidae,
603 Polycladida) in the Mediterranean basin. Redescription of the species *Leptoplana mediterranea*
604 (Bock, 1913) comb. nov. *Zootaxa* **56**, 45–56.
- 605 **Girstmair, J., Zakrzewski, A., Lapraz, F., Handberg-thorsager, M., Tomancak, P., Pitrone, P. G.,**
606 **Simpson, F. and Telford, M. J.** (2016). Light-sheet microscopy for everyone? Experience of
607 building an OpenSPIM to study flatworm development. *BMC Dev. Biol.* **16**, 1–16.
- 608 **Goette, A.** (1881). Zur Entwicklungsgeschichte der Würmer. *Zool. Anz.* **4**, 189–191.
- 609 **Gualda, E. J., Vale, T., Almada, P., Feijó, J. A., Martins, G. G. and Moreno, N.** (2013).
610 OpenSpinMicroscopy: An open-source integrated microscopy platform. *Nat. Methods* **10**, 599–
611 600.
- 612 **Halanych, K. M., Bacheller, J. D., Aguinaldo, A. M., Liva, S. M., Hillis, D. M. and Lake, J. A.** (1995).
613 Evidence from 18S ribosomal DNA that the lophophorates are protostome animals. *Science* (80-
614 .). **267**, 1641–1643.
- 615 **Hallez, P. P.** (1879). Contributions à l'histoire naturelle des Turbellariés. *Trav. l'Institut Zool. Lille la*
616 *Stn. Mari- time Wimereux* **2**, 1–213.

- 617 **Hartenstein, V. and Ehlers, U.** (2000). The embryonic development of the rhabdocoel flatworm
618 *Mesostoma lingua* (Abildgaard, 1789). *Dev. Genes Evol.* **210**, 399–415.
- 619 **Hejzol, A.** (2010). A twist in time—the evolution of spiral cleavage in the light of animal phylogeny.
620 *Integr. Comp. Biol.* **50**, 695–706.
- 621 **Hejzol, A., Obst, M., Stamatakis, A., Ott, M., Rouse, G. W., Edgecombe, G. D., Martinez, P., Baguñà,**
622 **J., Bailly, X., Jondelius, U., Wiens, M., Müller, W. E. G., Seaver, E., Wheeler, W. C., Martindale,**
623 **M. Q., Giribet, G. and Dunn, C. W.** (2009). Assessing the root of bilaterian animals with scalable
624 phylogenomic methods. *Proc. R. Soc. B Biol. Sci.* **276**, 4261–4270.
- 625 **Henry, J. J.** (1986). The role of unequal cleavage and the polar lobe in the segregation of
626 developmental potential during first cleavage in the embryo of *Chaetopterus variopedatus*.
627 *Roux's Arch. Dev. Biol.* **195**, 103–116.
- 628 **Henry, J. J.** (1989). Removal of the polar lobe leads to the formation of functionally deficient
629 photocytes in the annelid *Chaetopterus variopedatus*. *Roux's Arch. Dev. Biol.* **198**, 129–136.
- 630 **Henry, J. Q.** (2014). Spiralian model systems. *Int. J. Dev. Biol.* **58**, 389–401.
- 631 **Henry, J. J. and Martindale, M. Q.** (1987). The organizing role of the D quadrant as revealed through
632 the phenomenon of twinning in the polychaete *Chaetopterus variopedatus*. *Roux's Arch. Dev.*
633 *Biol.* **196**, 499–510.
- 634 **Henry, J. Q. and Martindale, M. Q.** (1998). Conservation of the spiralian developmental program: cell
635 lineage of the nemertean, *Cerebratulus lacteus*. *Dev. Biol.* **201**, 253–269.
- 636 **Henry, J. J. and Martindale, M. Q.** (1999). Conservation and innovation in spiralian development.
637 *Hydrobiologia* **402**, 255–265.
- 638 **Henry, J. Q., Perry, K. J. and Martindale, M. Q.** (2006). Cell specification and the role of the polar lobe
639 in the gastropod mollusc *Crepidula fornicata*. *Dev. Biol.* **297**, 295–307.
- 640 **Kato, K.** (1940). On the development of some Japanese polyclads. *Japanese J. Zool.* **8**, 537–574.
- 641 **Kaufmann, a., Mickoleit, M., Weber, M. and Huisken, J.** (2012). Multilayer mounting enables long-
642 term imaging of zebrafish development in a light sheet microscope. *Development* **139**, 3242–
643 3247.
- 644 **Kwan, K. M., Fujimoto, E., Grabher, C., Mangum, B. D., Hardy, M. E., Campbell, D. S., Parant, J. M.,**
645 **Yost, H. J., Kanki, J. P. and Chien, C.-B.** (2007). The Tol2kit: A multisite gateway-based
646 construction kit for Tol2 transposon transgenesis constructs. *Dev. Dyn.* **236**, 3088–3099.
- 647 **Lambert, J. D.** (2008). Mesoderm in spiralian: The organizer and the 4d cell. *J. Exp. Zool. Part B Mol.*
648 *Dev. Evol.* **310**, 15–23.
- 649 **Lambert, J. D.** (2009). Patterning the spiralian embryo: insights from *Ilyanassa*. In *Current topics in*
650 *developmental biology*, pp. 107–133. Elsevier Inc.
- 651 **Lambert, J. D.** (2010). Developmental patterns in spiralian embryos. *Curr. Biol.* **20**, R72–R77.
- 652 **Lambert, J. D. and Nagy, L. M.** (2001). MAPK signaling by the D quadrant embryonic organizer of the
653 mollusc *Ilyanassa obsoleta*. *Development* **128**, 45–56.
- 654 **Lambert, J. D. and Nagy, L. M.** (2003). The MAPK cascade in equally cleaving spiralian embryos. *Dev.*
655 *Biol.* **263**, 231–241.

- 656 **Lang, A.** (1884). *Die Polycladen (Seeplanarien) des Golfes von Neapel: und der angrenzenden Meeres-*
657 *Abschnitte: eine Monographie.* Leipzig: Leipzig, Verlag von Wilhelm Engelmann.
- 658 **Lapraz, F., Rawlinson, K. A., Girstmair, J., Tomiczek, B., Berger, J., Jékely, G., Telford, M. J. and Egger,**
659 **B.** (2013). Put a tiger in your tank: the polyclad flatworm *Maritigrella crozieri* as a proposed
660 model for evo-devo. *Evodevo* **4**, 1–15.
- 661 **Lehmann, F. E. and Hadorn, H.** (1946). Vergleichende Wirkungsanalyse von zwei antimitotischen
662 Stoffen, Colchicin und Benzochinon, am Tubifex-Ei. *Helv. Physiol. Pharmacol. Acta* **4**, 11–42.
- 663 **Li, R. and Albertini, D. F.** (2013). The road to maturation: somatic cell interaction and self-organization
664 of the mammalian oocyte. *Nat Rev Mol Cell Biol* **14**, 141–152.
- 665 **Lyons, D. C. and Henry, J. Q.** (2014). Ins and outs of spiralian gastrulation. *Int. J. Dev. Biol.* **58**, 413–
666 428.
- 667 **Malakhov, V. V. and Trubitsina, N. V.** (1998). Embryonic development of the polyclad turbellarian
668 *Pseudoceros japonicus* from the sea of Japan. *Russ. J. Mar. Biol.* **24**, 106–113.
- 669 **Marlétaz, F., Peijnenburg, K. T. C. A., Goto, T., Satoh, N. and Rokhsar, D. S.** (2019). A new spiralian
670 phylogeny places the enigmatic arrow worms among gnathiferans. *Curr. Biol.* **29**, 312–318.
- 671 **Martín-Durán, J. M. and Egger, B.** (2012). Developmental diversity in free-living flatworms. *Evodevo*
672 **3**, 1–22.
- 673 **Martindale, M. Q.** (1986). The ‘organizing’ role of the D quadrant in an equal-cleaving spiralian,
674 *Lymnaea stagnalis* as studied by UV laser deletion of macromeres at intervals between third and
675 fourth quartet formation. *Int. J. Invertebr. Reprod. Dev.* **9**, 229–242.
- 676 **Martindale, M. Q., Doe, C. Q. and Morrill, J. B.** (1985). The role of animal-vegetal interaction with
677 respect to the determination of dorsoventral polarity in the equal-cleaving spiralian, *Lymnaea*
678 *palustris*. *Wilhelm Roux’s Arch. Dev. Biol.* **194**, 281–295.
- 679 **Meshcheryakov, V.** (1991). *The common pond snail Lymnaea stagnalis.* In: “Animal species for
680 developmental studies Volume 1 Invertebrates” 69-131. 1st ed. (ed. Dettlaff, T.) and Vassetzky,
681 S.) Moscow: Springer.
- 682 **Meyer, N. P., Boyle, M. J., Martindale, M. Q. and Seaver, E. C.** (2010). A comprehensive fate map by
683 intracellular injection of identified blastomeres in the marine polychaete *Capitella teleta*.
684 *Evodevo* **1**, 8.
- 685 **Miller, A. L. and Bement, W. M.** (2009). Regulation of cytokinesis by Rho GTPase flux. *Nat. Cell Biol.*
686 **11**, 71–77.
- 687 **Nakama, A. B., Chou, H. C. and Schneider, S. Q.** (2017). The asymmetric cell division machinery in the
688 spiral-cleaving egg and embryo of the marine annelid *Platynereis dumerilii*. *BMC Dev. Biol.* **17**, 1–
689 22.
- 690 **Pick, K. S., Philippe, H., Schreiber, F., Erpenbeck, D., Jackson, D. J., Wrede, P., Wiens, M., Alié, A.,**
691 **Morgenstern, B., Manuel, M. and Wörheide, G.** (2010). Improved phylogenomic taxon sampling
692 noticeably affects nonbilaterian relationships. *Mol. Biol. Evol.* **27**, 1983–1987.
- 693 **Pित्रone, P. G., Schindelin, J., Stuyvenberg, L., Preibisch, S., Weber, M., Eliceiri, K. W., Huisken, J. and**
694 **Tomancak, P.** (2013). OpenSPIM - an open access platform for light sheet microscopy. *Nat.*
695 *Methods* **10**, 598–599.

- 696 **Rawlinson, K. A.** (2010). Embryonic and post-embryonic development of the polyclad flatworm
697 *Maritigrella crozieri*; implications for the evolution of spiralian life history traits. *Front. Zool.* **7**,
698 1–25.
- 699 **Rawlinson, K. A.** (2014). The diversity, development and evolution of polyclad flatworm larvae.
700 *Evodevo* **5**, 1–12.
- 701 **Rawlinson, K. A., Marcela Bolaños, D., Liana, M. K. and Litvaitis, M. K.** (2008). Reproduction,
702 development and parental care in two direct-developing flatworms (Platyhelminthes:
703 Polycladida: Acotylea). *J. Nat. Hist.* **42**, 2173–2192.
- 704 **Render, J. A.** (1983). The Second Polar Lobe of the Sabellaria cementarium Embryo Plays an Inhibitory
705 Role in Apical Tuft Formation. *Wilhelm Roux's Arch. Dev. Biol.* **192**, 120–129.
- 706 **Render, J. A.** (1989). Development of Ilyanassa obsoleta embryos after equal distribution of polar lobe
707 material at first cleavage. *Dev. Biol.* **132**, 241–250.
- 708 **Schindelin, J., Arganda-Carreras, I., Frise, E., Kaynig, V., Longair, M., Pietzsch, T., Preibisch, S.,**
709 **Rueden, C., Saalfeld, S., Schmid, B., Tinevez, J.-Y., White, D. J., Hartenstein, V., Eliceiri, K.,**
710 **Tomancak, P. and Cardona, A.** (2012). Fiji - an Open Source platform for biological image
711 analysis. *Nat. Methods* **9**, 676–682.
- 712 **Selenka, E.** (1881). *Zoologische Studien II. Zur Entwicklungsgeschichte der Seeplanarien.* Leipzig.
- 713 **Shibazaki, Y., Shimizu, M. and Kuroda, R.** (2004). Body handedness is directed by genetically
714 determined cytoskeletal dynamics in the early embryo. *Curr. Biol.* **14**, 1462–1467.
- 715 **Surface, F. M.** (1907). The early development of a polyclad, *Planocera inquilina*. *Proc. Acad. Nat. Sci.*
716 *Philadelphia* **59**, 514–559.
- 717 **Teshirogi, W., Sachiko, I. and Jatani, K.** (1981). On the Early Development of Some Japanese Polyclads.
718 *Rep. Fukaura Mar. Biol. Lab* **9**, 2–31.
- 719 **van den Biggelaar, J. A. M.** (1977). Development of Dorsoventral Polarity and Mesentoblast
720 Determination in *Patella vulgata*. *J. Morphol.* **154**, 157–186.
- 721 **van den Biggelaar, J. A. M.** (1996). Cleavage pattern and mesentoblast formation in Acanthochiton
722 crinitus (Polyplacophora, Mollusca). *Dev. Biol.* **174**, 423–430.
- 723 **van den Biggelaar, J. A. M. and Guerrier, P.** (1979). Dorsoventral polarity and mesentoblast
724 determination as concomitant results of cellular interactions in the mollusk *Patella vulgata*. *Dev.*
725 *Biol.* **68**, 462–471.
- 726 **Van den Biggelaar, J. A. M. and Guerrier, P.** (1983). *Origin of spatial organization.* In “*The Mollusca*”.
727 (ed. Wilbur, K. M.) San Diego, CA.
- 728 **Verdonk, N. H. and Van den Biggelaar, J. A. M.** (1983). *Early Development and the Formation of the*
729 *Germ Layers.* In: “*The Mollusca.*” 3rd ed. (ed. Wilbur, K. M.) San Diego, CA: 91-122.
- 730 **Wall, R.** (1990). *From oocyte to zygote.* In: “*This side up - spatial determination in the early*
731 *development of animals.*” (ed. Barlow, P.W., Bray, D., Green, P.B., Slack, J. M. W.) Cambridge:
732 Cambridge University Press 31-45.
- 733 **Wierzejski, A.** (1905). Embryologie von *Physa fontinalis* L. *Zeitschrift für wissenschaftliche Zool.* **83**,
734 502–706.

735 **Wilson, E. B.** (1898). Considerations on cell-lineage and ancestral reminiscence, based on a re-
736 examination of some points in the early development of annelids and polyclades. *Ann. N. Y. Acad.*
737 *Sci.* **11**, 1–27.

738 **Younossi-Hartenstein, A. and Hartenstein, V.** (2000). The embryonic development of the polyclad
739 flatworm *Imogine mcgrathi*. *Dev. Genes Evol.* **210**, 383–398.

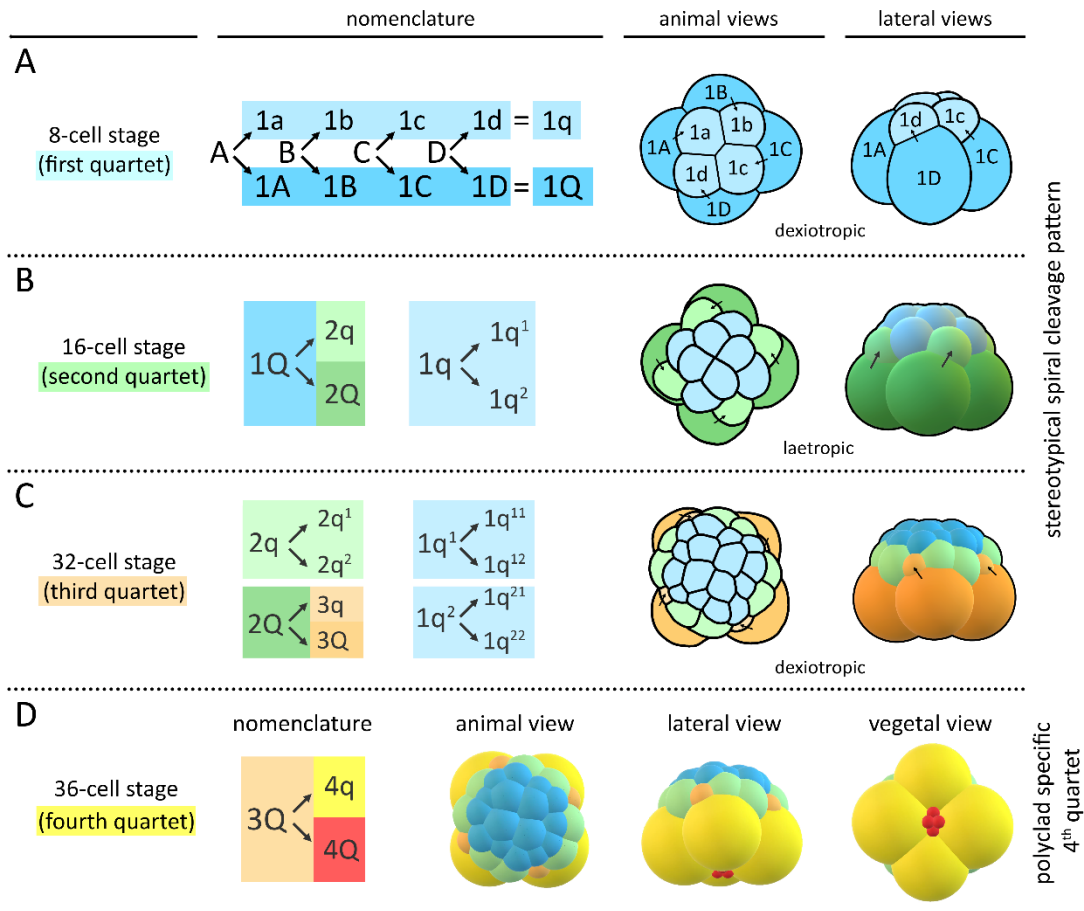
740

741 **List of abbreviations**

742 fluorinated ethylene propylene (FEP)
743 microtubule organizing centre (MTOC)
744 scanning electron microscopy (SEM)
745 selective plane illumination microscopy (SPIM)
746 spiral deformations (SD)
747 phosphate buffered saline (PBS)

748

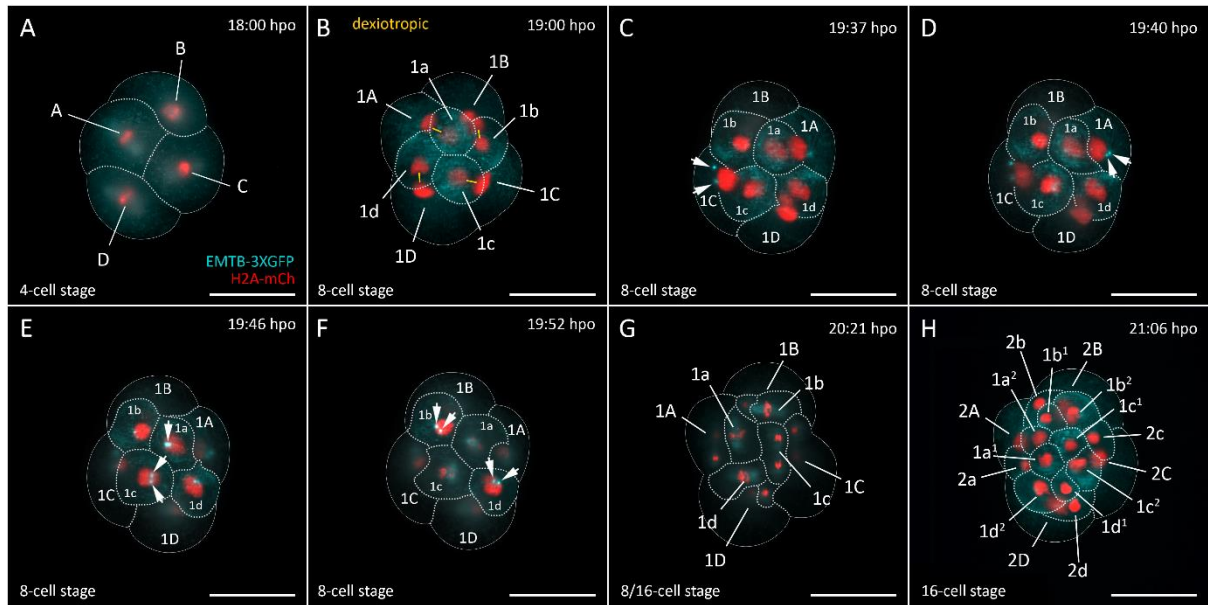
FIGURES



749

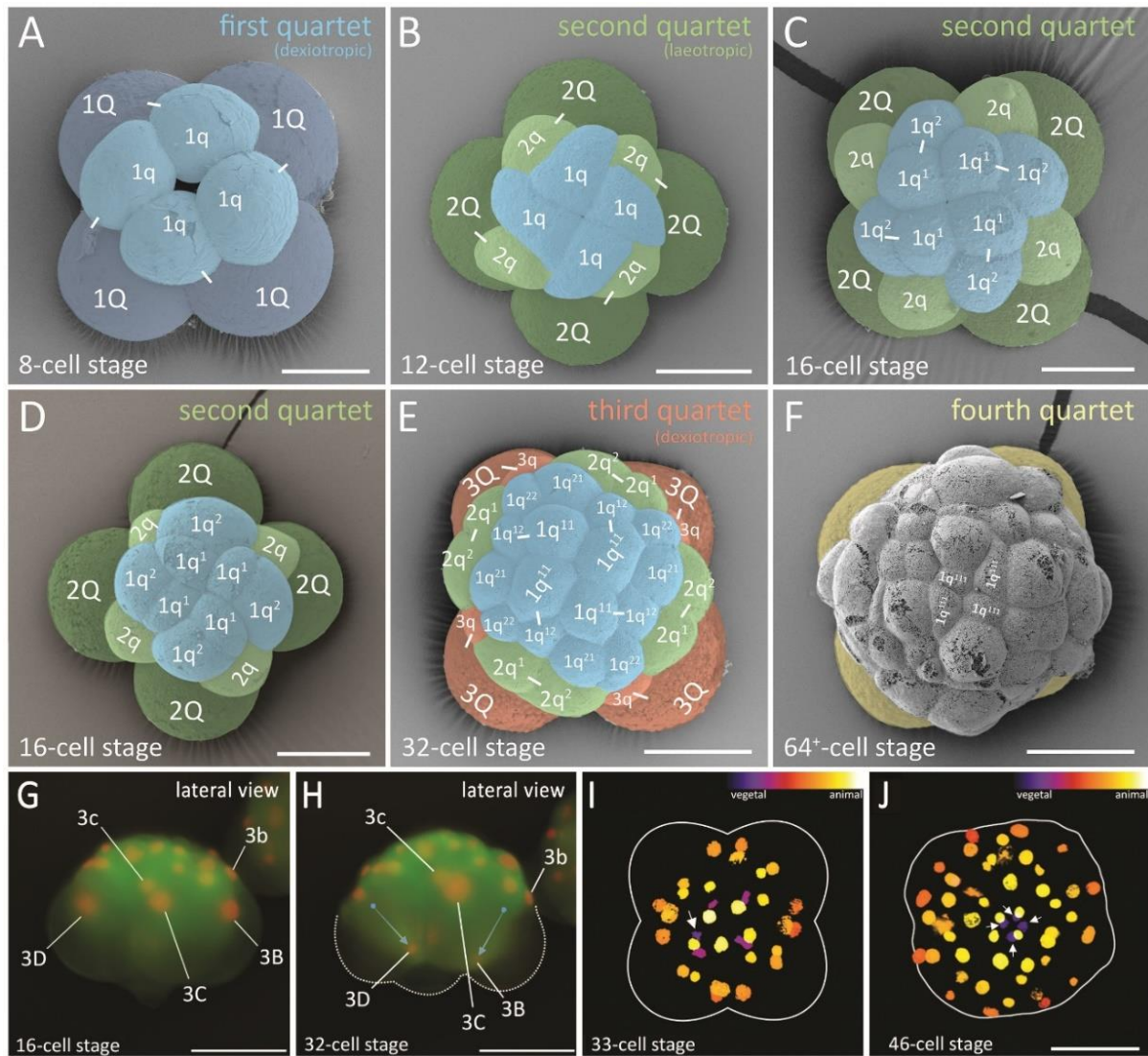
750 Figure 1 – Schematics and nomenclature of the spiral quartet cleavage as found in polyclad flatworms. Micromere
751 and macromere quartets (q and Q, respectively) are colour-coded. **(A)** The third cleavage (4- to 8-cell stage) is
752 unequal and asymmetric. The eight-cell stage embryo consists of four larger vegetal macromeres 1Q, and four
753 smaller animally positioned micromeres 1q sitting skewed to one side of their sister macromere, above the
754 macromeres' cleavage furrows. The typical spiral deformations (SD) of macromeres show a helical twist towards
755 one side with respect to the animal-vegetal axis. This is best seen if the embryo is viewed from the animal pole.
756 The resulting spiral shape taken by all four macromeres has been shown to be either clockwise (dexiotropic) or
757 counter clockwise (laetropic) among different lophotrochozoans. In the polyclad *M. crozieri* it is dexiotropic.
758 Notably it has been demonstrated that the mechanism of spiral deformations depends on actin filaments rather
759 than on spindle forming microtubules (Shibazaki et al., 2004). **(B-C)** In subsequent rounds of division, the larger
760 macromeres again divide unequally and asymmetrically sequentially forming the second and then the third quartets
761 of micromeres. During these divisions the spiral deformations appear in alternating dexiotropic/laetropic directions
762 (the rule of alternation) up to the fifth cleavage where a 32 cell-stage is reached. Up to this point, polyclad flatworms
763 represent a classic example of stereotypic lophotrochozoan spiral quartet cleavage. **(D)** The formation of the fourth

- 764 cleavage (4Q and 4q) deviates from the typical pattern seen in other spiral-cleaving embryos insofar as the
- 765 micromeres 4q become large and the macromeres 4Q diminutive. Q = A, B, C, D; q = a, b, c, d.



766

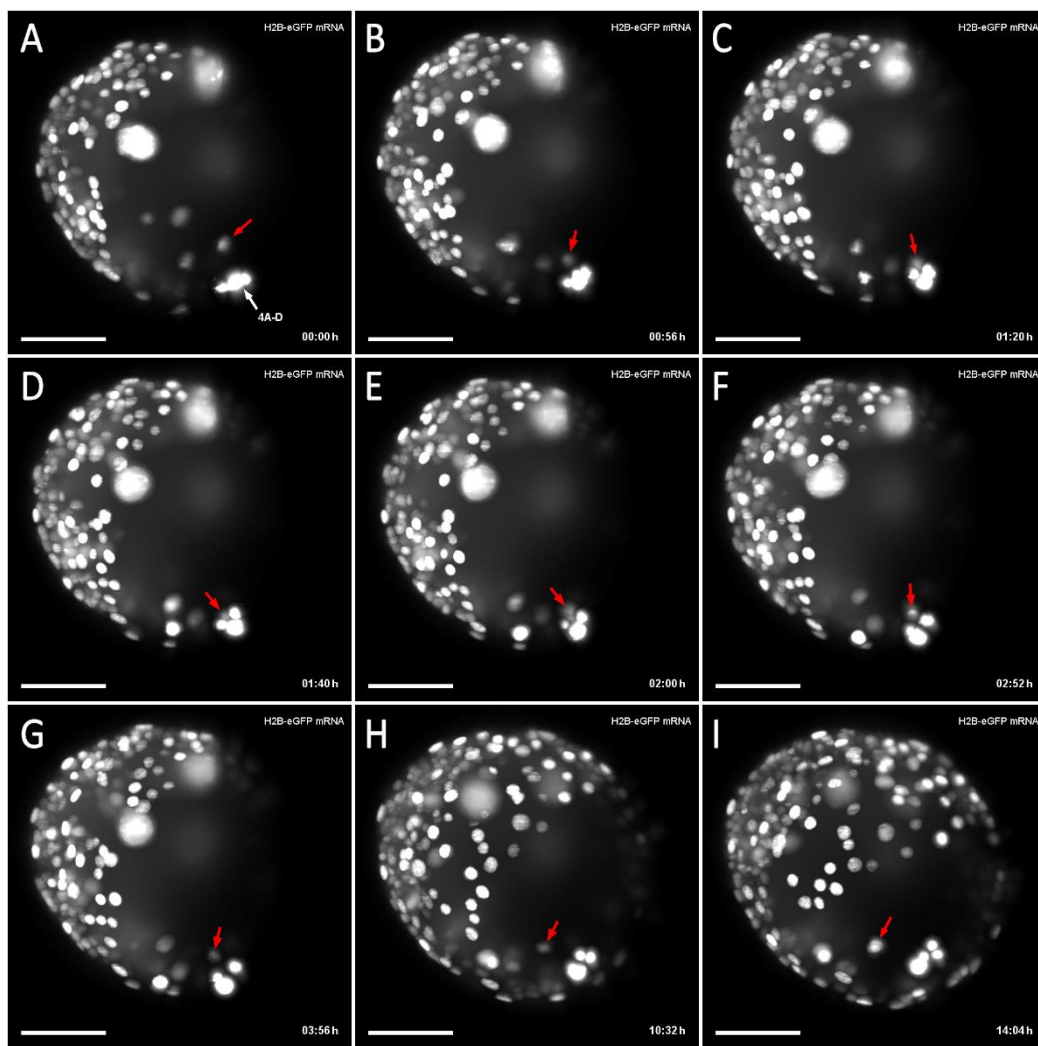
767 Figure 2 – Live-imaging of the transition from a 4-cell stage embryo to a 16-cell stage in *M. crozieri*. (A) 4-cell stage
 768 with pronounced animal and vegetal cross-furrow cells. (B-F) 8-cell stage preparing for the fourth cleavage round.
 769 White arrows point to the appearance of microtubule organizing centre (MTOC) (G) Divisions of the fourth cleavage
 770 round. (H) The embryo has reached the 16-cell stage is reached; hpo = hours post oviposition. Images captured
 771 with an OpenSPIM. Scalebar is 100 μm.



772

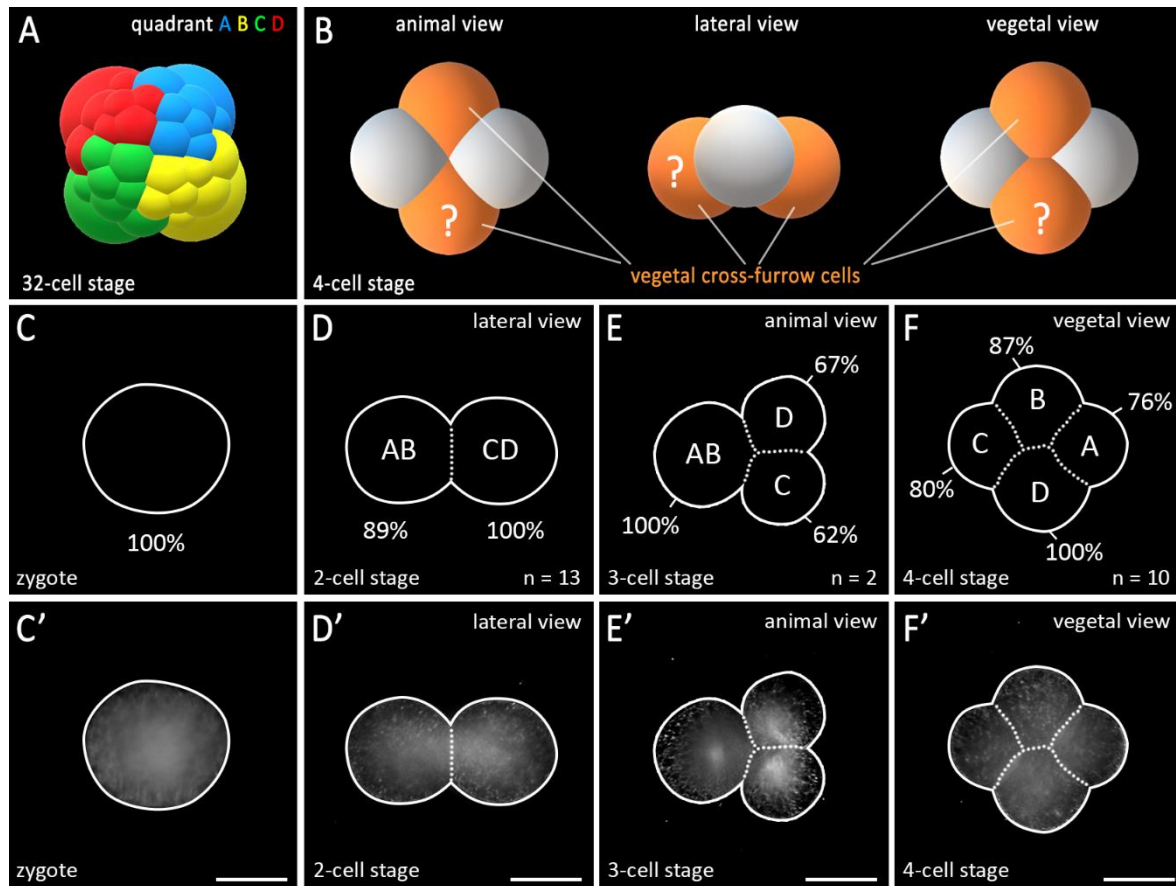
773 Figure 3 – Formation of the four quartets in *M. crozieri*. **(A-D)** SEM pictures coloured according to micromere
 774 quartets. **(A)** First quartet (1Q and 1q indicated in blue). **(B-D)** Second quartet (2Q and 2q) indicated in green. **(E)**
 775 Third quartet (3Q and 3q) indicated in orange. **(F)** Large fourth micromere quartet (4q) indicated in yellow. G-J:
 776 Formation of the fourth quartet **(G)** The 16-cell stage shows macromeres 3B-D and their nuclei at an animal position
 777 within the large blastomeres. **(H)** Same embryo as in G but at the 32-cell stage. Nuclei of 3B and 3D are now
 778 positioned at the vegetal pole of the macromeres. **(I)** 33-cell stage of a 3D reconstructed embryo (Their depth in
 779 the embryo is coded by colours as seen in top right part of the panel). Division of one of the four macromeres (3Q)
 780 into 4Q/4q has taken place. The white arrow indicates the newly formed small macromere of the fourth quartet
 781 (4Q) coloured purple indicating it is close to the vegetal pole. **(J)** 3D reconstructions showing that all four
 782 macromeres comprising the fourth quartet are now positioned at the most vegetal pole of the embryo (coloured
 783 purple and indicated by arrows). Scalebar in A-J = 50 μ m.

784



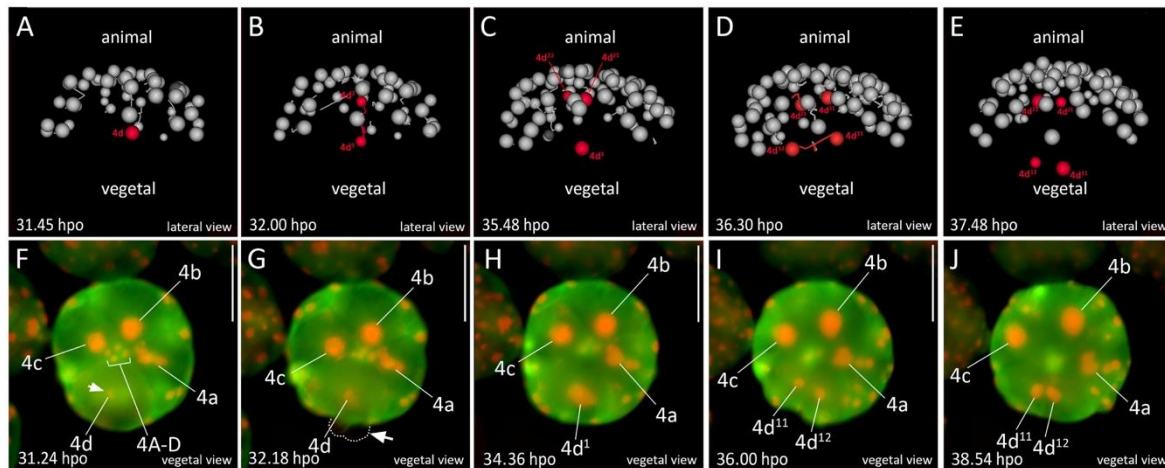
785

786 Figure 4 – Putative cell-cell interactions observed in the gastrulating polyclad flatworm *M. crozieri*. **(A-I)** A
787 descendant of cell 4d² (red arrow) is traced and can be seen approaching and later departing from small
788 macromeres 4A-D before epiboly is completed. Time represents hours (h) of time-lapse imaging; h is hours of
789 imaging with an OpenSPIM.. Scalebar = 50 μm.



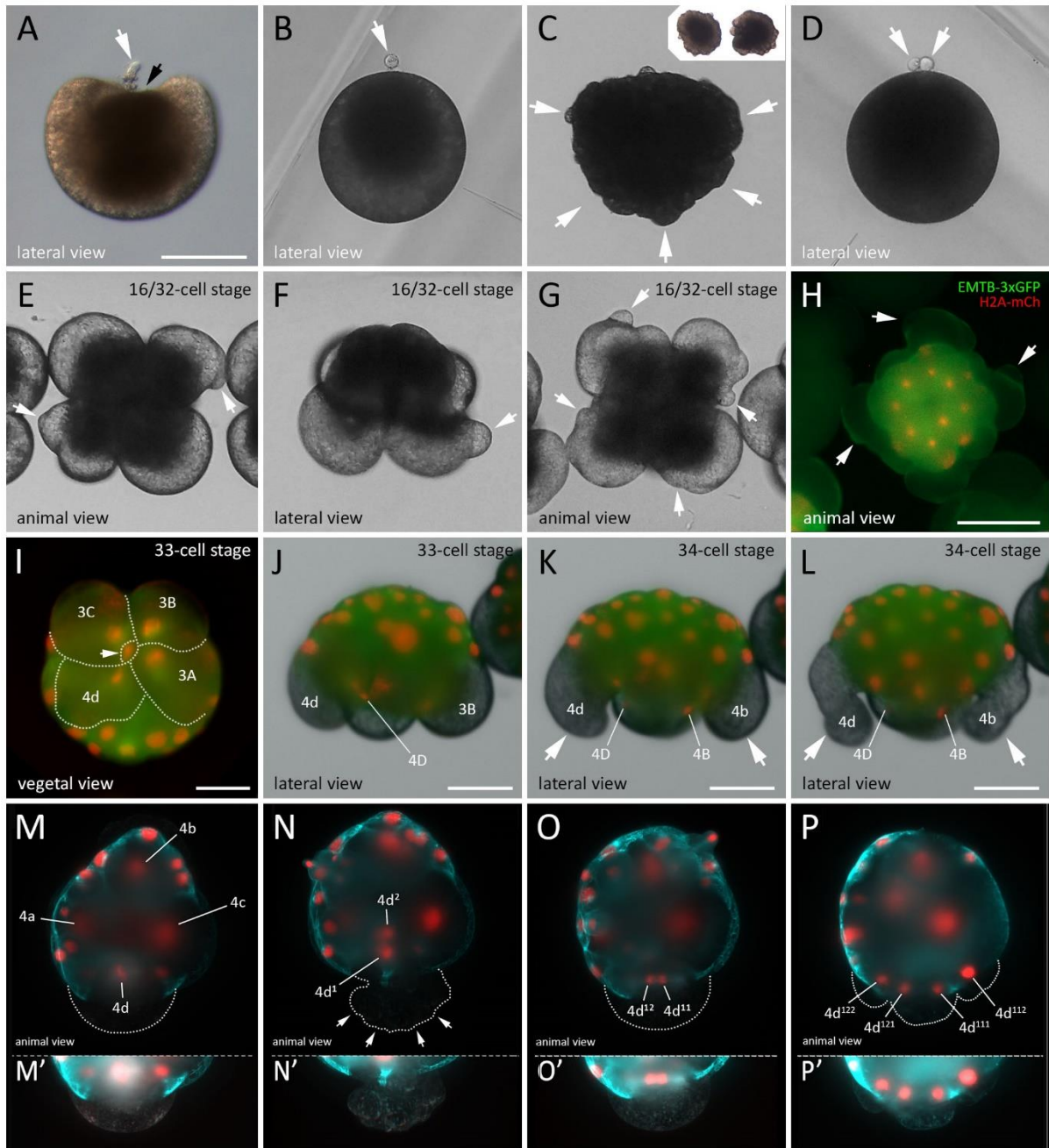
790

791 Figure 5 – Averaged volume measurements in *M. crozieri* blastomeres of the first and second cleavages. **(A)** A 3D
 792 model of a 4-cell stage embryo is depicted showing both vegetal cross-furrow cells that meet at the vegetal pole
 793 indicated in orange. **(B)** In unequal cleavers, one of the vegetal cross-furrow cells (depicted here in red) is already
 794 specified as the D quadrant at the 4-cell stage. Whether this is true for polyclad flatworms remains unclear, which
 795 is indicated here by a question mark. **(C)** A 3D model based on SEM pictures from *M. crozieri* embryos showing
 796 the four quadrants (A-D). **(D-H)** Volumes are given as a percentage of the volume of the total embryo, which is
 797 100%. **(F)** At the 2-cell stage the larger cell is assumed to represent blastomere CD and the smaller cell blastomere
 798 AB. **(G)** At the 3-cell stage blastomere CD most likely precedes the division of blastomere AB. **(H)** At the 4-cell
 799 stage the largest blastomere is always one of the vegetal cross-furrow cells and is interpreted as the D blastomere.
 800 **(D'-H')** All volume measurements come from 5-angle 3D multiview reconstructions and have been orientated with
 801 a view from their vegetal side. Only a single plane of the 3D reconstructed stack is shown. Scalebar = 100 μ m.



802

803 Figure 6 – Animal view of the cleavages of micromere 4d in *M. crozieri*. **(A-E)** The cleavage pattern of micromere
 804 4d (marked in red) is visualized using a 3D viewer (Fiji), showing in grey the position of all remaining nuclei except
 805 4A-D and 4a-4c. **(A)** Micromere 4d before its division. **(B)** Micromere 4d divides along the animal-vegetal pole and
 806 daughter cell 4d² is budded into the interior of the embryo and in close proximity to micromeres of the animal pole.
 807 **(C-E)** Both daughter cells of micromere 4d divide again, but this time both cells cleave meridionally **(F)** Micromere
 808 4d undergoes mitosis revealing the D quadrant. **(G)** The asymmetric division of micromere 4d along the animal-
 809 vegetal pole is barely visible but causes blebbing (arrow pointing at dashed line). **(H)** After the division, daughter
 810 cell 4d¹ remains large and is more vegetally positioned and therefore readily visible. 4d² is budded into the interior
 811 of the embryo, more animally positioned and cannot be seen anymore without optical sectioning. **(I-J)** Bilateral
 812 symmetry is clearly visible after the division of 4d¹. Oocytes were microinjected with nuclear marker H2A-mCherry
 813 (red) and microtubule marker EMTB-3xGFP (green) and the embryo used for 4d microscopy with OpenSPIM (A-
 814 E) or under a Zeiss Axio Zoom.V16 Stereo Microscope (F-J); hpo = hours post oviposition. Scalebar in images
 815 captured with the Axio Zoom = 100 μm.

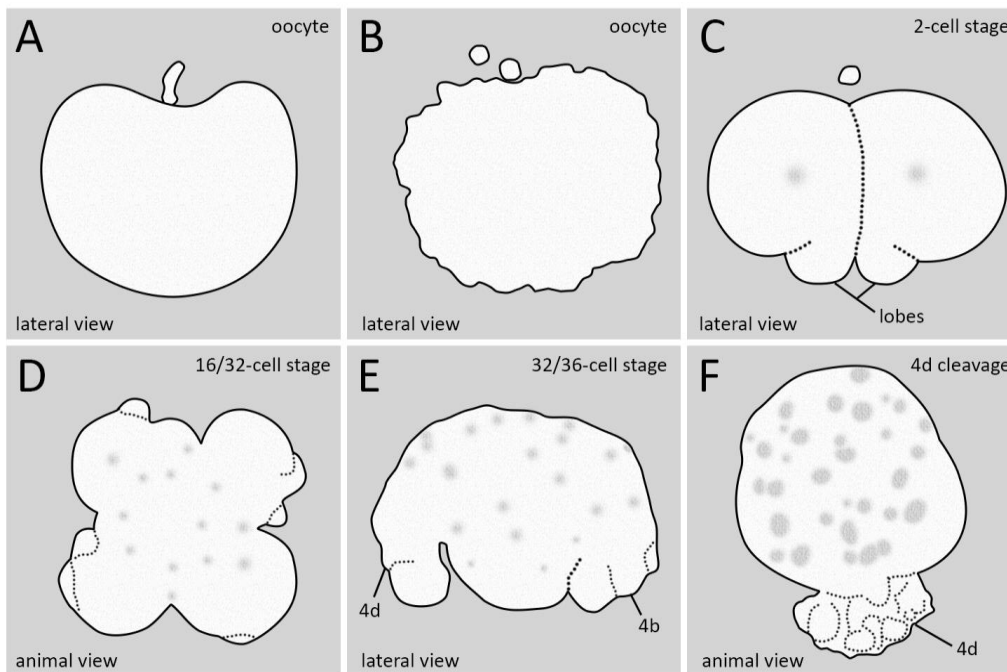


816

817 Figure 7 – Blebbing events during meiosis and spiral cleavage in the polyclad flatworm *M. crozieri* (A-D) Blebbing
 818 during egg maturation in *M. crozieri* oocytes. (A) Extrusion of first polar body (white arrow) and depression of the
 819 oocyte at the animal pole (black arrowhead). (B) Oocyte with one polar body and darkish pigment accumulated at
 820 the animal pole (C) Cell blebbing is recognisable by the formation of amoeboid/pseudopodia-like irregularities all
 821 over the cell membrane. (D) Egg cell with two polar bodies and darkish pigment accumulated at the animal pole.
 822 (E-L) Blebbing during the third and fourth quartet formation (E-H) Protrusions in the form of extracellular vesicle-
 823 like structures appear prior to third quartet formation (16-32-cell stage) among all four macromeres. (I-J) Vegetal
 824 (I) and lateral view (J) of the division of macromere 3D into tiny macromere 4D (white arrowhead). (K-L) Blebbing
 825 is accompanied by severe deformations of large micromeres 4b and 4d. (M-P) Animal view of the cleavages of

826 micromere 4d in *M. crozieri*. **(M)** Chromosome condensations are only visible in 4d. **(N)** Division of 4d is visible
 827 along the animal-vegetal axis of the embryo. White arrowheads show cytoplasmic perturbations during the
 828 cleavage of micromere 4d. **(O)** Meridional division of 4d¹ takes place. **(P)** The next division of the daughter cells of
 829 4d¹ is depicted. **(M'-P')** The 4d-cell and its progenies have been depicted separately below at increased exposure
 830 levels. Embryos with fluorescent signal were microinjected as oocytes with a microtubule marker (EMTB-3xGFP)
 831 and a histone nuclear marker (H2A-mCh). Live imaging was performed under a Leica DMI3000 B inverted
 832 scope (A-G), a Zeiss Axio Zoom.V16 Stereo Microscope (H-L) and an OpenSPIM (M-P). Scalebar is 100 µm in A
 833 and H, 50 µm in I-L, 100 µm in A and E and 50 µm in M-P.

834



835

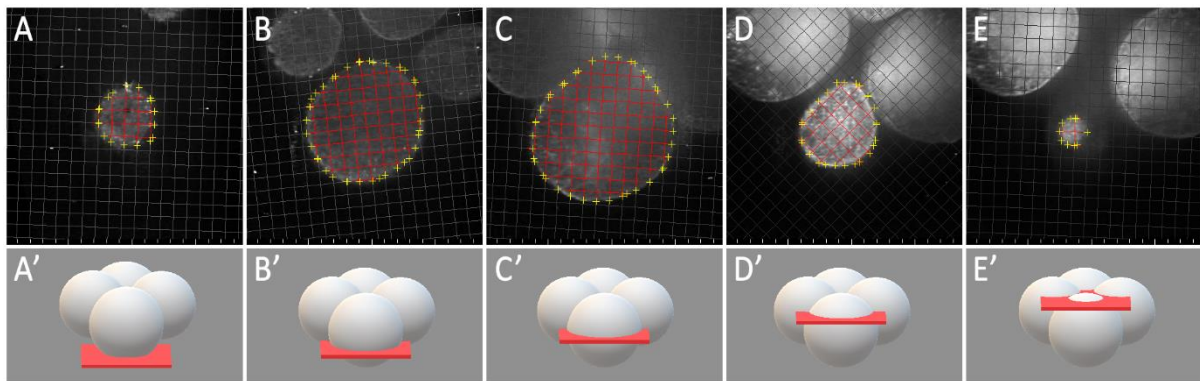
836 Figure 8 – Summary of cytoplasmic perturbations described in different polyclad flatworm species. **(A)** Depression
 837 of the animal pole during the formation of the first polar body described by Kato (1940) for some Japanese polyclad
 838 species and for *Maritigrella crozieri* (this study). **(B)** Cell blebbing in oocytes as described for most polyclads during
 839 the first and second meiotic divisions (see Gammoudi et al. 2012). **(C)** Vegetal lobe like structures found in
 840 *Pseudostylochus intermedius* (Teshirogi & Sachiko, 1981) and *Pseudoceros japonicus* (Malakhov and Trubitsina,
 841 1998). Drawing taken from *P. intermedius* **(D)** Cytoplasmic perturbations seen in *Pseudostylochus intermedius* (8-
 842 to 16-cell stage) (Teshirogi & Sachiko, 1981) and *Maritigrella crozieri* (16- to 32-cell stage, this study). **(E)** Waves
 843 of contractile activity in all four macromeres of *Maritigrella crozieri* (this study) whereby macromeres attain an
 844 elongated shape. **(F)** Similar cytoplasmic perturbations seen during the highly asymmetric cleavage of micromere
 845 4d found in *Maritigrella crozieri* (this study).

846 ADDITIONAL FILES

847 Additional file 1 – 50 min OpenSPIM movie of the third cleavage in an embryo of *M. crozieri* with labeled nuclei
848 (H2B:GFP) showing spiral deformations (SD) and dextrorotatory cleavage.

849 Additional file 2 – Putative cell-cell interactions captured with an OpenSPIM of an embryo undergoing epiboly. It
850 can be observed how nuclei of the small macromeres (4A-4D) get in very close proximity with nuclei of close
851 descendants of micromere 4d² for a short period of time and then goes away.

852



853

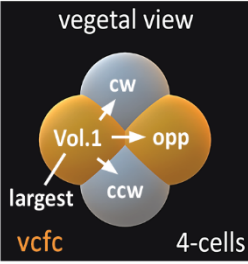
854 Additional file 3 – An example of volume measurements performed on a 4-cell stage polyclad flatworm embryo,
855 showing only 5 representative slices within a Z-stack (the original file contains hundreds of slices after image
856 processing is completed).

***Maritigrella crozieri* volume measurements (in μm^3)**

2-cell stages	Vol.1	Vol.2	total
Mc_E01	1937900	1896000	3833900
Mc_E02	2221600	1999899	4221499
Mc_E03	2228000	2099300	4327300
Mc_E04	2467300	2009100	4476400
Mc_E05	2438100	1518600	3956700
Mc_E06	2219200	1794100	4013300
Mc_E07	1831600	1779900	3611500
Mc_E08	1626900	1594200	3221100
Mc_E09	1609300	1574700	3184000
Mc_E10	1640500	1564500	3205000
Mc_E11	1550800	1419200	2970000
Mc_E12	2311800	1884800	4196600
Mc_E13	1620000	1537600	3157600

3-cell stages	Vol.1	Vol.2 (ccw)	Vol.3 (cw)	total
Mc_E01	1486400	925760	941850	3354010
Mc_E02	879360	629110	533000	2041470

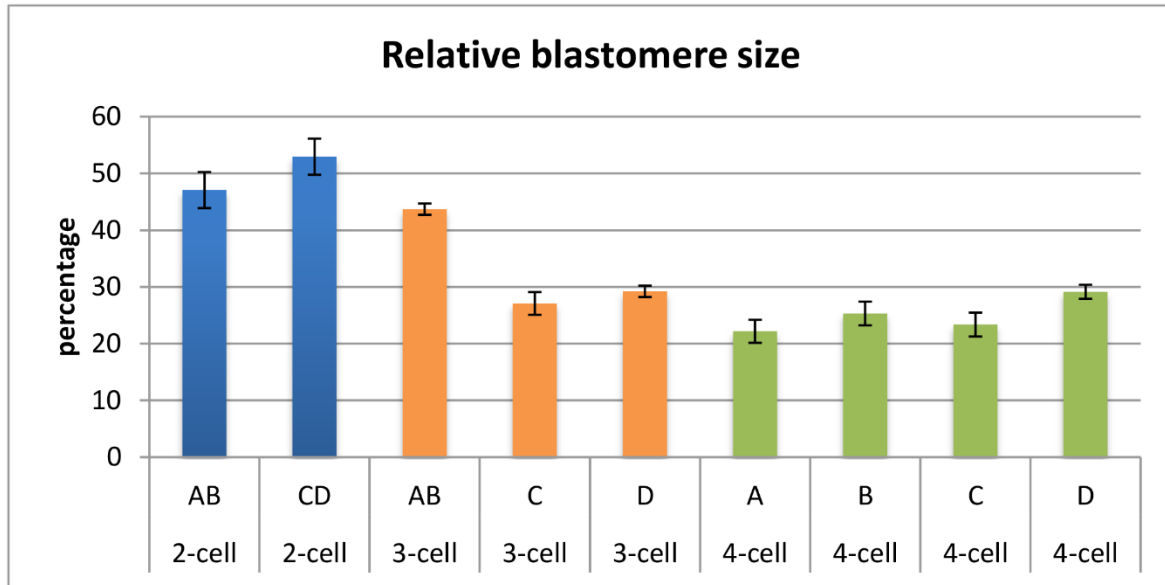
4-cell stages	vcfc?	Vol.1	Vol.2 (ccw)	Vol.3 (opp)	Vol.4 (cw)	total
Mc_E01	yes	1146600	846790	1142700	999380	4135470
Mc_E02	yes	1063700	760500	916010	846790	3587000
Mc_E03	yes	1105200	856540	936490	975000	3873230
Mc_E04	yes	1171500	801940	899930	939900	3813270
Mc_E05	?	1049600	970610	780980	928200	3729390
Mc_E06	yes	919430	842890	861900	751240	3375460
Mc_E07	yes	1185600	784420	999900	1013600	3983520
Mc_E08	yes	524570	381240	486060	434380	1826250
Mc_E09	yes	894600	688380	758090	610860	2951930
Mc_E10	yes	982350	709830	906790	610860	3209830



857

858 Additional file 4 – Table of blastomere volume measurements in 2-, 3- and 4-cell stages. Vol.1 indicates the largest
 859 blastomere. In 2-cell stages Vol.2 accounts for its sister cell. In 4-cell stages Vol.2 corresponds to cells positioned
 860 clockwise (cw) of it, Vol. 3 to the cell opposite of it (opp) and Vol.4 counter clockwise (ccw) of it (see schematic
 861 embryo inset). The vegetal cross-furrow-cells (vcfc) are shown in orange.

862

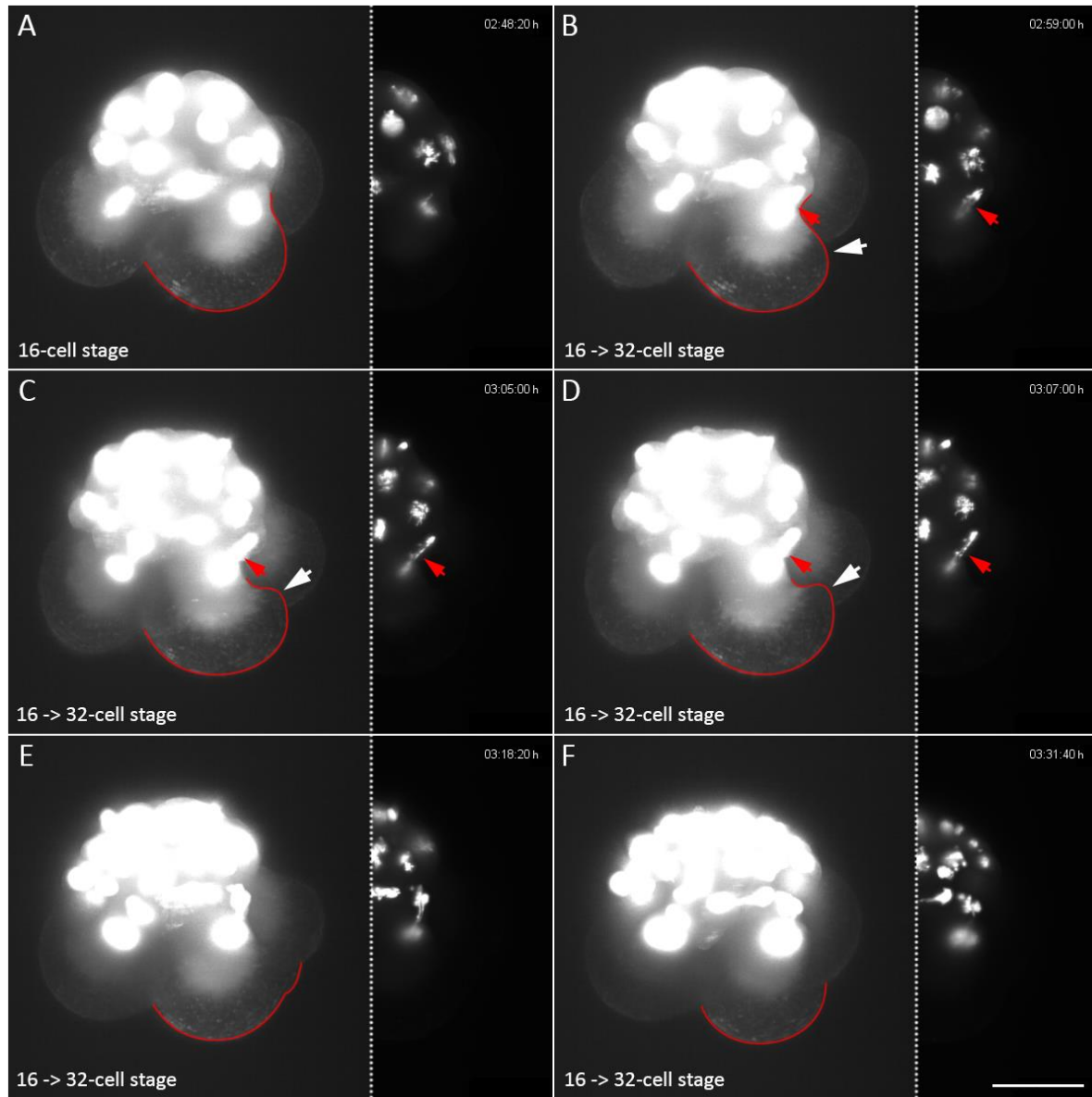


863

864 Additional file 5 – An average of the volume measurements of 3D reconstructed blastomeres in *M. crozieri* embryos
865 of the 2-cell, 3-cell and 4-cell stages. The data are based on measurements of individual blastomeres. To provide
866 the data as percentages makes sense as each individual embryo can vary in size. The 2-cell stages are indicated
867 as blue columns (n=13), 3-cell stages as orange (n=2) and 4-cell stages as green columns (n=13). Volumes are
868 given as a percentage of the total volume of the embryo which is 100%. Standard deviations are indicated for
869 smaller blastomeres only. In two-cell stages a 6% difference was noted between the two cells on average. The
870 larger blastomere has been designated as CD. In 3-cell stages the two sister blastomeres (C and D) have a larger
871 volume than the remaining sister cell and have been designated as C and D according to a slight volume difference.
872 In 4-cell stages the largest blastomere is one of the vegetal cross-furrow cells and has been indicated as D. It is
873 5.8% larger compared to its sister cell indicated as C. Of the two, remaining sister blastomeres, the size difference
874 is only 3.3% with the larger one indicated as blastomere B. Error bars indicate standard error of the mean.

875 Additional file 6 – The initial division pattern of micromere 4d using live-imaging data from an Axio Zoom.V16
876 (Zeiss). The 4d blastomere does not divide laterally but first divides along the animal-vegetal axis into a smaller,
877 animally positioned cell, which we designate as 4d¹ and a larger, vegetally positioned cell, we designate 4d²

878

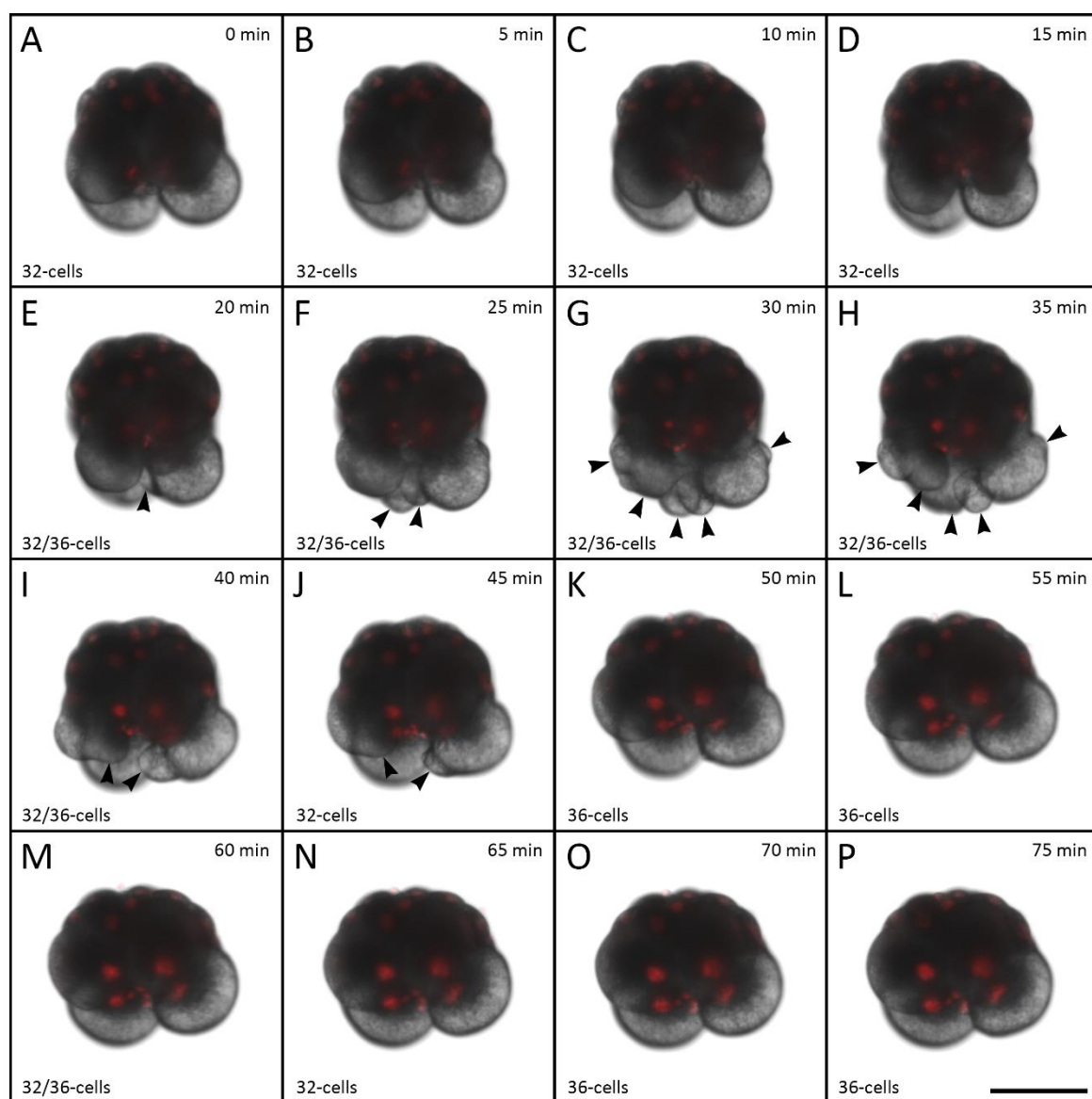


879

880 Additional file 7 – Cytoplasmic perturbations imaged with the OpenSPIM in one of the second quartet macromeres
881 shown during mitosis. The whole embryo is shown over-exposed to better visualize the membranous outlines of
882 the macromeres. To the right of each embryo, the nuclei are depicted with normal exposure. Red arrows point to
883 the same nucleus of the embryo. A red line highlights the outline of the corresponding macromere. The shape
884 deformations caused by the cytoplasmic perturbations of the macromere correlate precisely with the mitotic
885 anaphase and reach a maximum in panel D. Scalebar = 50 μm .

886 Additional file 8 – Movie of and embryo forming the third quartet. Prior to the cleavage of macromeres 2A-2D,
887 blebbing becomes visible on their cell surfaces in form of small, vesicle-like protrusions. The movie shows that
888 mitotic cytoskeletal activity during anaphase correlates with the observed protrusions.

889



890

891 Additional file 9 – (A-P) Time-lapse recording showing the formation of the small macromeres (4Q) and large
892 micromeres (4q) of a single *M. crozieri* embryo in 5 min intervals showing striking cytoplasmic perturbation activity
893 at the vegetal pole of the embryo (indicated by black arrows). (F-K) 25 min of cytoplasmic perturbations are clearly
894 visible in macromeres 3A-3D. Live imaging was performed under a Zeiss Axio Zoom.V16 Stereo Microscope. Scale
895 bar is 100 μ m.